



**HAL**  
open science

# Transcription-based circadian mechanism controls the duration of molecular clock states in response to signaling inputs

Sofia Almeida, Madalena Chaves, Franck Delaunay

► **To cite this version:**

Sofia Almeida, Madalena Chaves, Franck Delaunay. Transcription-based circadian mechanism controls the duration of molecular clock states in response to signaling inputs. *Journal of Theoretical Biology*, 2020, 484, pp.110015. 10.1016/j.jtbi.2019.110015 . hal-02299359

**HAL Id: hal-02299359**

**<https://hal.science/hal-02299359>**

Submitted on 21 Dec 2021

**HAL** is a multi-disciplinary open access archive for the deposit and dissemination of scientific research documents, whether they are published or not. The documents may come from teaching and research institutions in France or abroad, or from public or private research centers.

L'archive ouverte pluridisciplinaire **HAL**, est destinée au dépôt et à la diffusion de documents scientifiques de niveau recherche, publiés ou non, émanant des établissements d'enseignement et de recherche français ou étrangers, des laboratoires publics ou privés.



Distributed under a Creative Commons Attribution - NonCommercial 4.0 International License

# Transcription-based circadian mechanism controls the duration of molecular clock states in response to signaling inputs

Sofia Almeida<sup>a,b,\*</sup>, Madalena Chaves<sup>a,\*</sup> and Franck Delaunay<sup>b,\*</sup>

<sup>a</sup>1600 Université Côte d'Azur, Inria, INRA, CNRS, UPMC Univ Paris 06, Biocore team, Sophia Antipolis, France

<sup>b</sup>Université Côte d'Azur, CNRS, INSERM, iBV, France

## ARTICLE INFO

### Keywords:

mammalian clock model; transcriptional regulation; calibration; *tau* mutation; circadian alignment.

## ABSTRACT

The molecular oscillator of the mammalian circadian clock consists in a dynamical network of genes and proteins whose main regulatory mechanisms occur at the transcriptional level. From a dynamical point of view, the mechanisms leading to an oscillatory solution with an orderly protein peak expression and a clear day/night phase distinction remain unclear. Our goal is to identify the essential interactions needed to generate phase opposition between the activating CLOCK:BMAL1 and the repressing PER:CRY complexes and to better distinguish these two main clock molecular phases relating to rest/activity and fast/feeding cycles. To do this, we develop a transcription-based mathematical model centered on linear combinations of the clock controlled elements (CCEs): E-box, R-box and D-box. Each CCE is responsive to activators and repressors. After model calibration with single-cell data, we explore entrainment and period tuning via interplay with metabolism. Variation of the PER degradation rate  $\gamma_p$ , relating to the *tau* mutation, results in asymmetric changes in the duration of the different clock molecular phases. Time spent at the state of high PER/PER:CRY decreases with  $\gamma_p$ , while time spent at the state of high BMAL1 and CRY1, both proteins with activity in promoting insulin sensitivity, remains constant. This result suggests a possible mechanism behind the altered metabolism of *tau* mutation animals. Furthermore, we expose the clock system to two regulatory inputs, one relating to the fast/feeding cycle and the other to the light-dependent synchronization signaling. We observe the phase difference between these signals to also affect the relative duration of molecular clock states. Simulated circadian misalignment, known to correlate with insulin resistance, leads to decreased duration of BMAL1 expression. Our results reveal a possible mechanism for clock-controlled metabolic homeostasis, whereby the circadian clock controls the relative duration of different molecular (and metabolic) states in response to signaling inputs.

## 1. Introduction

In the vast majority of organisms the circadian clock is a fundamental mechanism that governs daily behavior and cell physiology providing adaptation to external changes. In mammals, coordination between cycles of rest/activity and fast/feeding with the external light/dark cycle is ensured by a complex and hierarchical timing system: in brief, a hypothalamic central clock receives light inputs and in turn coordinates clocks in peripheral tissues and cells along the 24 h cycle via internal signaling. Both central and peripheral clocks share the same molecular makeup.

Experimental studies and mathematical models have uncovered a dynamical network of clock components. The core clock mechanism consists of the CLOCK:BMAL1 protein complex that promotes transcription of *Per* and *Cry* mRNA. The PER:CRY protein complex subsequently formed in the cytoplasm then translocates into the nucleus where it both blocks CLOCK:BMAL1 transcriptional activity and displaces the CLOCK:BMAL1 heterodimer from its cognate promoters (Ye et al., 2014). Another negative feedback loop between CLOCK:BMAL1 and REV-ERB $\alpha$  is also a part of the core clock mechanism (Buhr and Takahashi, 2013), (Relógio et al., 2011). In spite of the phase differences between core clock mRNAs and core clock proteins not being exactly the same, specific peak order between the core clock components, such as BMAL1, REV-ERB $\alpha$ , PER and CRY occurs already at the mRNA level (Koike et al., 2012).

Endogenous circadian clocks coordinate gene activation patterns and protein concentrations that oscillate in individual cells with a 24 hour period, such that different times of day are characterized by different cellular protein

\*Corresponding author

 [sofia.jf.almeida@gmail.com](mailto:sofia.jf.almeida@gmail.com) (S. Almeida); [madalena.chaves@inria.fr](mailto:madalena.chaves@inria.fr) (M. Chaves);

[Franck.Delaunay@univ-cotedazur.fr](mailto:Franck.Delaunay@univ-cotedazur.fr) (F. Delaunay)

 <http://www-sop.inria.fr/members/Madalena.Chaves/> (M. Chaves); <http://ibv.unice.fr/research-team/delaunay/>

(F. Delaunay)

ORCID(s):

profiles. Of particular importance is the antiphasic relation between CLOCK:BMAL1 and PER:CRY that strongly correlates with the day/night separation. We note that the terminology “phase” is formally used as to denote the angle of rotation of the oscillator relative to a reference value. However, by abuse of language, throughout this article we sometimes use “phase” in a more general sense, to designate a given stage of the molecular circadian oscillation, as for instance to refer to an activating phase (when CLOCK:BMAL1 is up and PER:CRY is down) or to a repressing phase (with CLOCK:BMAL1 down and PER:CRY up).

A combination of experimental and computational approaches has helped increase knowledge on the circadian clock. Goodwin proposed in 1975 a model based on a simple negative feedback loop between a protein and its own gene (Goodwin, 1965). Such a feedback loop was indeed uncovered, first in *Drosophila* (Zehring et al., 1984) and later in other organisms (Bell-Pedersen et al., 2005). Since then a number of dynamic modeling studies have furthered the discussion on the mammalian cellular clock (see Podkolodnaya et al. (2017) for a comparative review). Examples of these models are (Leloup and Goldbeter, 2003), (Forger and Peskin, 2003), (Relógio et al., 2011), and (Yan et al., 2014), that present varying ways of studying the system. Moreover, (Mirsky et al., 2009) propose a model that purposely minimizes post-translation modified species and (Becker-Weimann et al., 2004) focus on clock modeling using a reduced number of species. Applications of clock models are useful for studying the interconnection between the mammalian clock and other essential cellular processes, such as the cell cycle (Gérard and Goldbeter, 2012), (Zámborszky et al., 2007), (Feillet et al., 2015), (Bieler et al., 2014) and metabolism (Woller et al., 2016), (Woller and Gonze, 2018).

In this work, we first aim to investigate whether major mammalian clock properties such as oscillation, orderly protein peak expression and CLOCK:BMAL1/PER:CRY phase opposition can be recovered by a short transcription-based model that includes the majority of the core clock components and uses simple equation modeling terms. Thus, unlike large models, such as that of (Leloup and Goldbeter, 2003), that recover antiphasic oscillation of CLOCK:BMAL1 and PER:CRY in the context of comprehensive clock modeling, we aim here to uncover a reduced set of interactions that allow to recover this property. For this, we have focused on the clock controlled elements (CCEs): E-box, D-box and R-box. Some previous models have also represented the effect of CCEs on the clock: (Korenčič et al., 2012) focus exclusively on regulation between CCE modulation factors, proposing independent competition between CCEs modeled by a multiplicative relation, and (Jolley et al., 2014) highlight the role of D-box in a model that reproduces expected timing of CRY1 peak expression.

In our model, we simultaneously minimize the number of variables and restrict post-translational modifications to the PER:CRY mediated transrepression. While post-transcriptional mechanisms, including RNA-based mechanisms, are essential for the proper functioning of the clock, this doesn't mean these mechanisms are dynamically significant for oscillation or for the correct order of protein peak expression, as their contribution may be in the creation of specific delays that in a modeling perspective can be achieved by adjusting parameters on the essential dynamical interactions. In fact, transcription/translation feedback loops are usually shorter than circadian periods and delays such as that of PER degradation or that of PER nuclear entry via phosphorylation are known to contribute to the 24 h circadian period (Gallego and Virshup, 2007). Thus, our model is built on a view of the mammalian clock system working, most significantly, as an integrator of signals at the transcriptional level. The general assumption behind this simplistic modeling is that there are always sufficient amounts of rate-limiting active enzymes to carry out the essential post-translational modifications.

Our model reproduces the expected order of peak expression of the core clock proteins: BMAL1, then PER2, then CRY1 (Koike et al., 2012), as well as the aimed antiphasic relation between BMAL1 and PER:CRY. Model calibration is achieved by fitting to high temporal resolution REV-ERB $\alpha$  expression data from single cells, (Feillet et al., 2014), and we verify robustness of the oscillatory behavior to changes of parameters. We then seek to study the interplay between clock and metabolism, without including metabolic modeling directly, but rather from the point of view of the integration and response to metabolic and light -related signals by the clock network. As such, we start by analyzing the system with and without an extra self-regulatory loop representative of the impact of the E-box controlled transcriptional coactivator PGC1- $\alpha$  on ROR activity and observe the period response of the mammalian cellular clock to the parameters governing this interaction. Furthermore, we verify that this internal control loop increases the entrainment region of the clock to an external signal. Additionally, the system presents a type I phase response curve to an additive input on PER expression. Next, we investigate the *tau* mutation by varying the PER degradation rate. This mutation observed in hamsters and mice results in altered clock period and metabolism. We discover that the average duration of peak expression changes differently for each clock protein. From this, we hypothesize that the time spent at different clock phases, mainly at the activating CLOCK:BMAL1 and the repressing PER:CRY phases, is relevant for metabolic outcomes. We further test our hypothesis by studying the system's response to the alignment/misalignment state of

fast/feeding and light/dark signals. Results show an opposite trend between the duration of CLOCK:BMAL1 and PER:CRY. Finally, we hypothesize and discuss a relation between the time spent at different molecular clock phases and the duration of cellular states of insulin sensitivity and resistance.

## 2. Model Design, Calibration and Robustness

To construct a concise yet biologically meaningful mathematical model, we use ODEs and favor mass action kinetic terms as well as Michaelis-Menten and low exponent Hill function ( $n = 2$ ) terms that reasonably describe complex formation. This is in agreement with experimentation, where cooperative binding of clock proteins to target genes hasn't been observed (Smolen and Byrne, 2009). Furthermore, we restrict post-translational effects to protein natural degradation, formation/dissociation of the PER:CRY complex and nuclear export of the CLOCK:BMAL1:PER:CRY complex, and focus instead on transcriptional details. Thus, the model is centered on the competition of pairs of transcription factors in binding to certain specific regions of genome: the clock controlled elements (CCEs). These CCEs are the E-box (enhancer box) activated by CLOCK:BMAL1 whose promoter activity can be blocked by CRY binding, the R-box (REV-ERB $\alpha$ /ROR response element) activated by ROR and repressed by REV-ERB $\alpha$  and the D-box activated by DBP, HLF and TEF and repressed by E4BP4 (see Table 11).

Here, we focus on understanding the minimal mechanisms for orderly clock protein expression, in particularly the antiphase oscillation between CLOCK:BMAL1 and PER2/PER:CRY. We base our choice of CCEs on the work of (Ueda et al., 2005) showing which CCEs are sufficient to guarantee clock rhythmicity in phase with PER2 and antiphase with BMAL1. Other experimental results point to more extensive clock networks. For instance, (Yang et al., 2013) found three functional E-boxes at the REV-ERB promoter, (Yamamoto et al., 2004) show the presence of R-box elements in DBP and REV-ERB promoters as well as a higher number of CCEs in general and (Ukai-Tadenuma et al., 2011) present substantial evidence for a D-box in combination with R-box at the CRY1 promoter. Fig. 1 shows a scheme of the molecular mechanisms and interactions included in our model.

We start by deriving appropriate equations to describe the effect of each CCE (E-box, D-box and R-box), which include an activator with a positive effect and a repressor with a negative effect, that compete for binding. Independent competition as in the R-box and D-box cases (Fig. 11) is well described by multiplying the terms of activation and repression. This insures adequate modeling of active repression in the blocking of activators as well as the positive definiteness of gene activation rates. As for the E-box, CRY binds to a previously bound BMAL1 on the target gene, blocking its promoter activity rather than directly blocking the gene itself, and the competition is not independent.

Furthermore, BMAL1 promoter activity is assumed to represent the CLOCK:BMAL1 complex, as their transcriptional regulation is similarly achieved by 1 R-box and BMAL1 is rate-limiting in the formation of CLOCK:BMAL1 (Lefta et al., 2011). DBP is representative of all D-box activators. The equations for the three CCEs are shown in Eqs 1, 2 and 3:

$$E_{box} = V_E \frac{[BMAL1]}{[BMAL1] + k_E + k_{Er}[BMAL1][CRY]} \quad (1)$$

$$R_{box} = V_R \frac{[ROR]}{[ROR] + k_R} \frac{k_{Rr}^2}{k_{Rr}^2 + [REV]^2} \quad (2)$$

$$D_{box} = V_D \frac{[DBP]}{[DBP] + k_D} \frac{k_{Dr}}{k_{Dr} + [E4BP4]} \quad (3)$$

In our model we consider independent multiplicative competition between the terms of the majority of pairs of activator/repressor of each CCE, but additive relations between the contributions of each CCE to gene promoters, as has been observed for the activation of the *mPer1* promoter by DBP and CLOCK:BMAL1 (Yamaguchi et al., 2000). The model is shown in Eqs. (4) to (11): the eight variables are the 3 pairs of activators/repressors mentioned above

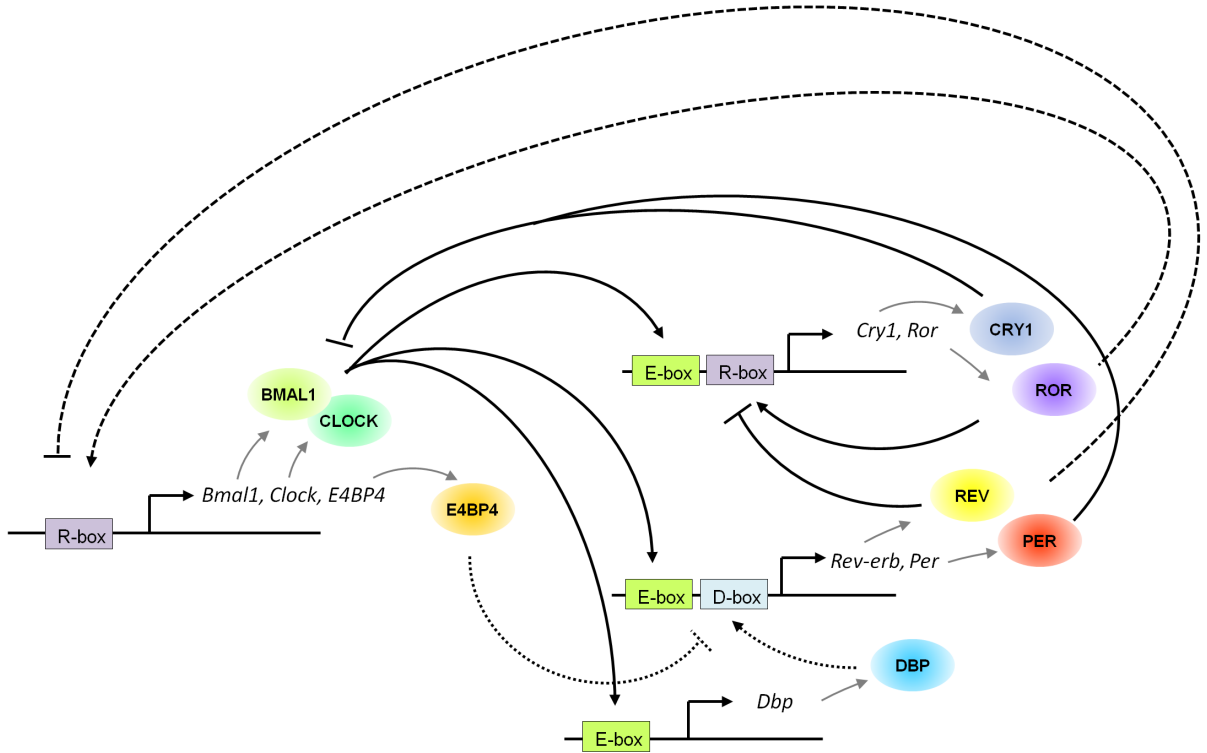


**Figure 1: Simplified molecular mechanisms of the mammalian circadian clock.** The CLOCK:BMAL1 protein complex promotes transcription of *Per*, *Cry*, *Ror*, *Rev-erb* and *Dbp* via E-boxes. CRY1 and PER:CRY block CLOCK:BMAL1 transcriptional activity, forming the main transcription-translation feedback loop. RORs (activators) and REV-ERBs (repressors) compete for R-box binding, coordinating expression of *Clock*, *Bmal1*, *E4BP4*, *Ror* and *Cry1*. Finally, D-box, activated by DBP and repressed by E4BP4, also contributes for expression of *Rev-erb* and *Per*.

(Equations (1) to (3)) as well as PER and the PER:CRY complex. All variables directly represent the rate of change of protein concentrations.

$$\frac{d[BMAL1]}{dt} = R_{box} - \gamma_{bp}[BMAL1][PER : CRY] \quad (4)$$

$$\frac{d[ROR]}{dt} = E_{box} + R_{box} - \gamma_{ror}[ROR] \quad (5)$$

$$\frac{d[REV]}{dt} = 2E_{box} + D_{box} - \gamma_{rev}[REV] \quad (6)$$

$$\frac{d[DBP]}{dt} = E_{box} - \gamma_{db}[DBP] \quad (7)$$

$$\frac{d[E4BP4]}{dt} = 2R_{box} - \gamma_{E4}[E4BP4] \quad (8)$$

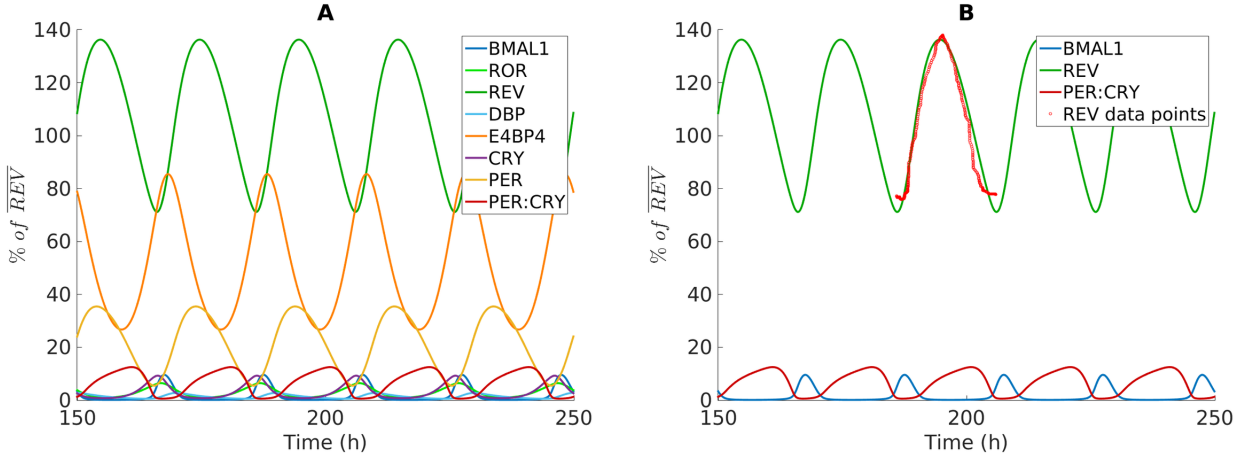


**Figure 2: The mammalian circadian clock can be described by a model focused on transcriptional regulation.** Output of the mammalian circadian clock model for parameters of Table 1. A) Oscillation of all eight model variables; T = 20.1 h. B) BMAL1 and PER:CRY have an antiphasic relation; calibration of the model using data from (Feillet et al., 2014) (Fig. 1, Panel A) for a peak of REV-ERB $\alpha$  in mouse fibroblast cells (NIH-3T3) – a filter was applied to smooth the data.

$$\frac{d[CRY]}{dt} = E_{box} + 2R_{box} - \gamma_{pc}[PER][CRY] + \gamma_{cp}[PER : CRY] - \gamma_c[CRY] \quad (9)$$

$$\frac{d[PER]}{dt} = E_{box} + D_{box} - \gamma_{pc}[PER][CRY] + \gamma_{cp}[PER : CRY] - \gamma_p[PER] \quad (10)$$

$$\frac{d[PER : CRY]}{dt} = \gamma_{pc}[PER][CRY] - \gamma_{cp}[PER : CRY] - \gamma_{bp}[BMAL1][PER : CRY] \quad (11)$$

where the negative term  $-\gamma_{bp}[BMAL1][PER : CRY]$  represents the nuclear export of CLOCK:BMAL1 via complex formation with PER:CRY and the terms  $\gamma_{pc}[PER][CRY]$  and  $\gamma_{cp}[PER : CRY]$  represent formation and dissociation of the PER:CRY complex respectively. The model includes the two step mechanism of the repression of CLOCK:BMAL1 by PER:CRY (Ye et al., 2014), with CRY also being a repressor of BMAL1 activity on E-box (Equation 1). Furthermore, note that the variables CRY and ROR directly model CRY1 and RORc, via the appropriate combination of CCEs, see (Ueda et al., 2005), even though we take them as representative of all CRYs and RORs.

Fig. 2 A) shows a solution of the model for the calibrated parameters (see Table 1). The model fits well to the high temporal resolution experimental data for relative fluorescence intensities of VENUS-tagged REV-ERB $\alpha$  protein obtained from (Feillet et al., 2014) (Fig. 2 B). We collected data from Fig. 1, Panel A of (Feillet et al., 2014), applied a filter to remove irregularities and normalized these data as percentage of the REV-ERB $\alpha$  mean value (% of REV). This normalization allows to better compare our results with the experimental data obtained in single-live-cell imaging of REV-ERB $\alpha$ ::VENUS, that measures relative levels of protein expression (Feillet et al., 2014). The fit is obtained via an optimization based on non-linear cost minimization, with the use of matlab's *fminsearch* command. All parameters result from the minimization of the distance of the REV variable to data points. The period of the system converges to the period of the data (T = 20.1 h). We can observe phase opposition between CLOCK:BMAL1 and PER:CRY, the property of interest (Fig. 2 A). The phase relation between CLOCK:BMAL1 and REV-ERB $\alpha$  (Fig. 2 B) of 7.1 h is also in agreement with experimental observation (Ko and Takahashi, 2006).

Moreover, Fig. 3 shows a zoom on the proteins of the main TTFL: an appropriate phase separation occurs for BMAL1, PER, CRY1 and PER:CRY. Note that all modeling terms have low Hill coefficient  $n$ , with the majority being

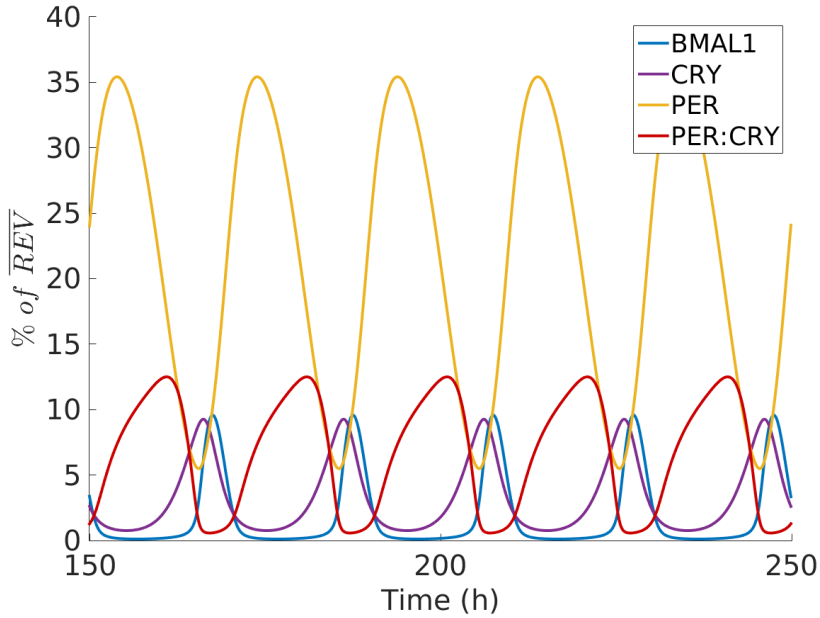


**Figure 3: Oscillation of the main TTFL clock proteins.** Orderly expression of clock proteins is in accordance with experimental observation: BMAL1, then PER, then CRY1; BMAL1 and PER:CRY are in phase opposition.

Michaelis-Menten terms, except the repression achieved by REV-ERB $\alpha$ . In the case of REV-ERB $\alpha$ , active repression occurs via recruitment of co-repressor to genes, which requires two REV-ERB $\alpha$  molecules; monomer REV-ERB $\alpha$  binding is not sufficient for active gene repression acting exclusively as an inhibitor of ROR binding (Everett and Lazar, 2014) (Zamir et al., 1997). REV-ERB $\alpha$  monomer repression may indeed be what happens at gene promoters where R-boxes are not in close proximity (Crumbley et al., 2010), however, here we assume REV-ERB $\alpha$  active repression and study the model with  $n = 2$ , respecting the stoichiometry of co-repressor activation. Nevertheless, simulations for  $n = 1$  yield the same order of protein peak expression as simulations with  $n = 2$ .

In summary, the modeling framework here developed is a tool that can be used for dynamic modeling of genetic networks of this type. It consists in describing protein rates of change as a combination of independent responses to certain regulatory regions of the genome, which in turn are modeled so as to describe the competition between activators and repressors.

Moreover, we verify the robustness of oscillations to perturbations in its parameters as shown by the sensitivity analysis in Fig. 12. Each parameter is varied by 20% around the calibrated point and oscillations are never lost although the period may change, which suggests period tuning is possible within a range of 18 - 23 h approximately. We can observe that parameters such as  $V_R$  and  $\gamma_{db}$  impact on the period the most, while variations on, for instance,  $k_{Er}$  and  $\gamma_{bp}$  have little impact. In general R-box promotes longer periods, as parameters that lead to an increase in R-box value,  $V_R$  and  $k_{Rr}$ , have a positive effect on the period. Similarly D-box promotes shorter periods and E-box has a very mild effect on the period (with  $V_E$  and  $k_{Er}$  having opposite effects). Additionally, the increase in the rate of complex formation  $\gamma_{pc}$  leads to an increase in the clock period and unsurprisingly the rate of complex dissociation  $\gamma_{cp}$  has an opposite effect, meaning that favoring the repressor PER:CRY favors longer periods – as such the rate of formation of the BMAL1:PER:CRY complex  $\gamma_{bp}$  that favors the removal of both the repressor PER:CRY and the activator BMAL1 has almost no effect on clock period. Finally, the increase in PER degradation rate  $\gamma_p$  leads to shorter periods, while its decrease lengthens the period, which is consistent with the S662G mutation in humans leading to FASPS syndrome.

### 3. Chromatin remodeling by CLOCK:BMAL1 as an internal mechanism of period control

Recently, more relevance has been attributed to the role of CLOCK:BMAL1 in promoting a transcriptionally permissive chromatin state for other transcription factors, allowing to integrate sensors of cellular energy status and nu-

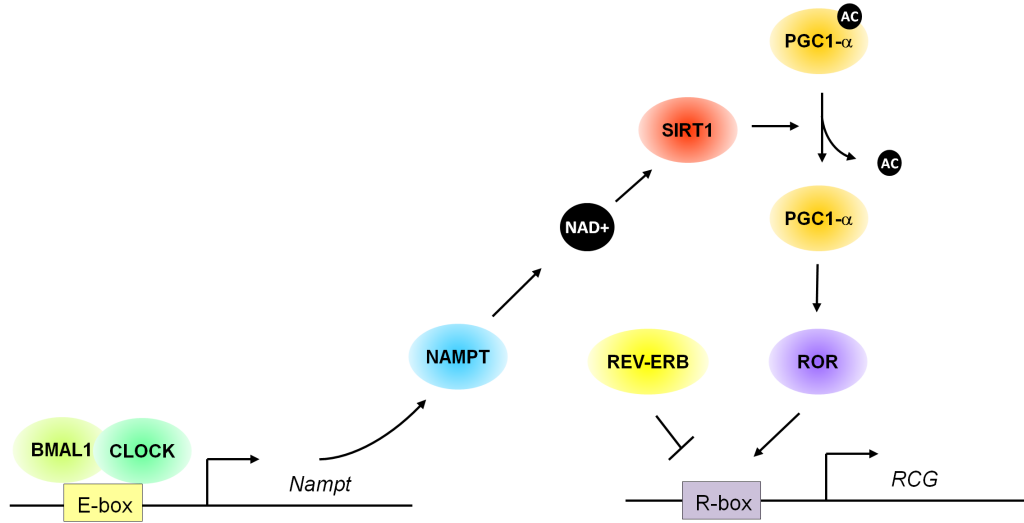


**Figure 4: PGC1- $\alpha$  integrates cellular metabolism and the mammalian circadian clock.** CLOCK:BMAL1 promotes PGC1- $\alpha$  indirectly by promoting expression of SIRT1 and the rate-limiting enzyme NAMPT which generates the cofactor NAD<sup>+</sup>, via E-boxes. Upon binding to NAD<sup>+</sup>, SIRT1 deacetylates PGC1- $\alpha$ . Deacetylated PGC- $\alpha$  then co-activates ROR which in turn antagonizes REV-ERB repressing activity thereby turning on R-box controlled genes (RCG).

trient availability with the molecular clock (Trott and Menet, 2018).

From a modeling point of view, this means that CLOCK:BMAL1 may be rhythmically altering specific model parameters that reflect chromatin states, thus acting as a closed-loop control mechanism that modulates one or more specific parameters.

In the previous section, in order to ensure that our model represents an autonomous oscillatory clock, we have taken a constant value for parameters that can potentially be affected by the interplay with the cell's energy metabolism. Now, we investigate whether a biologically derived function representative of the oscillatory chromatin permissiveness state could be used to tune a parameter. The circadian clock oscillates with a period close to 24 hours, but is observed to vary in a larger range, from 18 to 26 hours approximately (see (Saini et al., 2012) and (Feillet et al., 2014)). As indicated by our sensitivity analysis, parameters representing R-box activity are very relevant for period tuning. Thus, we investigate the implication of these parameters in chromatin remodeling in the real system and whether it's possible to adequately modulate them by metabolic inputs in our model.

Biologically, PGC1- $\alpha$  appears as an important transcription coactivator that facilitates ROR connection to the genome at the R-box binding site. CLOCK:BMAL1 can possibly promote PGC1- $\alpha$  in more than one way, particularly by promoting expression of the NAMPT enzyme (Ramsey et al., 2009) and the sirtuin SIRT1 (Zhou et al., 2014) via E-boxes: NAMPT is rate-limiting in the biosynthesis of NAD<sup>+</sup> that acts as a cofactor of SIRT1, which deacetylates and activates PGC1- $\alpha$  (Tang, 2016). This control loop is shown in Fig. 4.

Thus, PGC1- $\alpha$  activity on R-box is a good candidate to represent the oscillatory chromatin status. As such, we design the non-linear control  $\mu$  by considering PGC1- $\alpha$  to be given by an E-box ( $PGC1-\alpha = E\text{-box}$ ) and its activity as a facilitator of the binding of ROR to R-box to be expressed as acting on the parameter  $k_R$  of R-box, by making  $k_R \rightarrow \mu k_R$  in Equation 2, where  $\mu$  is given by:

$$\mu = V_1 \frac{k_1}{k_1 + E\text{box}} \quad (12)$$

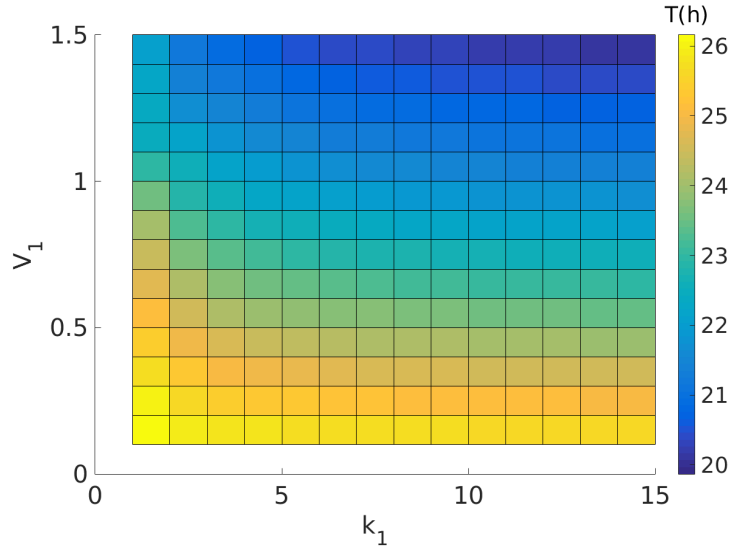


**Figure 5: Tuning of the period with the internal loop  $\mu$ .** Variations in the period of the system with the parameters  $V_1$  and  $k_1$  of  $\mu$  (Eq. 12). In this region the system behaves with the exact same features of Fig. 2. Outside of this region the system presents complex behavior.

Thus R-box becomes:

$$R_{box} = V_R \frac{[ROR]}{[ROR] + V_1 \frac{k_1}{k_1 + E_{box}} k_R} \frac{k_{Rr}^2}{k_{Rr}^2 + [REV]^2} \quad (13)$$

An adjustment of the parameter  $V_R$  allows to enter a region where the period can be controlled via the  $\mu$  internal loop, without altering the system's dynamical behavior, as intended. Thus, illustrating the ability of the clock system in incorporating metabolic signals. Fig. 5 shows the period of the system for variations of  $V_1$  and  $k_1$ , when period control is achieved via  $\mu$ . Outside this region the system behaves in a complex manner. Setting  $V_R = 50$  allows to be in the region of period control. The remaining parameters are unchanged as shown in Table 1.

Thus, introducing chromatin remodeling increases the model's period range in a robust way. The fact that a biologically-derived closed-loop function allows period control and doesn't interfere with the qualitative dynamical behavior of the system illustrates one of the many ways in which the circadian clock is able to tune and integrate signals via internal loops in order to optimize circadian output, i.e. the system has the ability to regulate itself via this function. The period-control response to the internal closed-loop function highlights the ability of our model to correctly include chromatin remodeling terms. We make  $V_1 = 0.41$  and  $k_1 = 10$  (with  $V_R = 50$ ) to take the period of the oscillator to 24 h and will from now on work with this tuned system and explore its response to external signals.

#### 4. Phase Response Curves and Entrainment

A particularly important characteristic of the circadian clock is its ability to synchronize to external signals, as well as the phase response induced by an external input pulse. In order to explore these properties and validate our model, an input  $I_{pulse}$  is added in the equation of the PER protein, such as  $\frac{d[PER]}{dt} = I_{pulse} + E_{box} + D_{box} - \gamma_{pc}[PER][CRY] + \gamma_{cp}[PER : CRY] - \gamma_p[PER]$ . The idea is to mimic the PER promoter's response in transducing a variety of external signals such as stress hormones (So et al., 2009), (Tamaru et al., 2011), (Reddy et al., 2012).

Fig. 6 shows the phase-response curve (PRC) of the system when we make a temporary perturbation on PER: the transient phase-shift is measured when the phase of the perturbation is varied over the course of one circadian cycle. For this, we consider the first BMAL1 peak that occurs after the perturbation and compute the difference between the time at which this peak occurs in the perturbed and non-perturbed cases. Duration of the pulse is two hours. Data

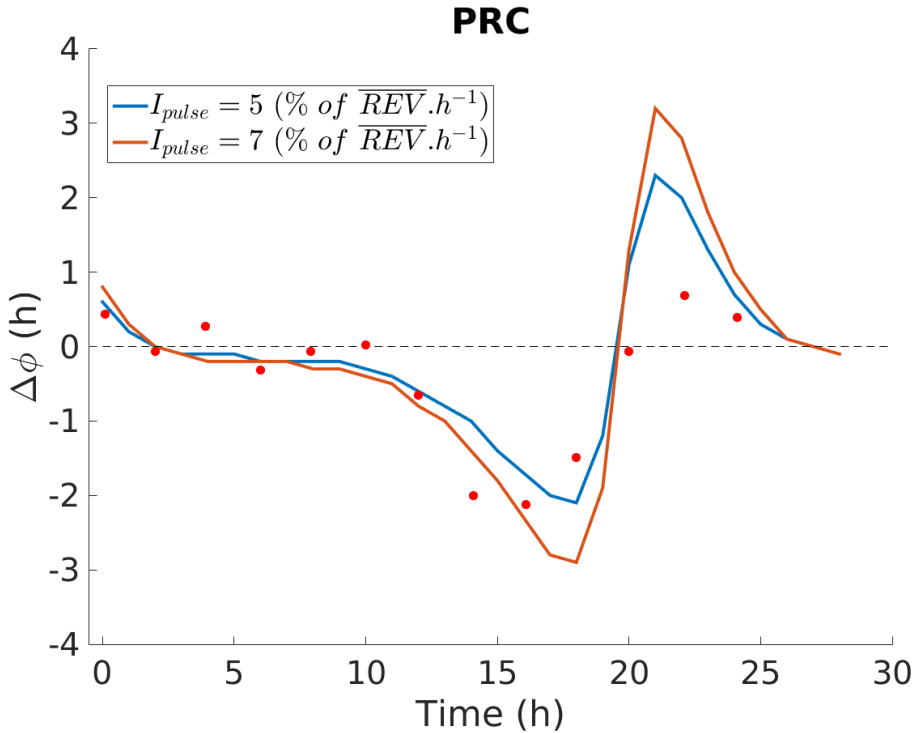


**Figure 6: Phase response curves.** Phase response curves of the system (measured as the phase shift in BMAL1) to two external pulses of different intensities, acting via stimulation of PER expression. Data points from Pendergast et al., (2010), of photic entrainment in wild-type mice are shown for comparison (Pendergast et al., 2010). The duration of the pulses is 2 h.

from (Pendergast et al., 2010) for photic entrainment in wild type mice, are shown for comparison. Our simulation shows a type I PRC, for two pulse intensities  $I_{pulse}$ , with shape similar to those of wild type mice, with the delay zone being larger than the advance zone. The majority of organisms typically have PRCs of this type, illustrating an ability to synchronize to external signals. Observe that phase shifts are more pronounced for higher intensity pulses.

We next analyze the entrainment of our model to a sinusoidal and to a rectangular wave, for different periods and amplitudes. In Fig. 7 we observe that, for both the sinusoidal (Fig. 7 A) and the rectangular (Fig. 7 B) waves, the region of entrainment forms a characteristic shape known as the Arnold tongue with entrainment becoming possible for larger period ranges with increasing amplitude. Entrainment with a sinusoid in general allows for larger regions of entrainment than with a square wave, a result that is obtained experimentally in observations of photic entrainment in hamsters (Boulos et al., 2002), as well as in numerical simulations of both photic (Gonze and Goldbeter, 2000) and temperature (Heiland et al., 2012) entrainment in circadian clocks. Entrainment via a sinusoidal wave leads to some points of period doubling, where the ratio between the period of the clock and that of the entraining signal is 2:1, as well as one point where the ratio between periods becomes 3:1. Rectangular waves also allow for a couple of points where the period of the clock becomes three times the period of the entraining wave.

Furthermore, Fig. 13 shows the same simulation for the model without the closed loop control mechanism introduced above in Equation 12. The closed-loop control increases the region of entrainment of the system by an external oscillatory input, thus revealing a possible role of chromatin remodeling in improving the ability of clock entrainment to signals.

## 5. Asymmetric variations in the duration of molecular clock phases on the *tau* mutation.

We now investigate the model dynamics under changes of the PER degradation rate  $\gamma_p$ . Changing this parameter may relate experimentally to observations in animal models of the *tau* mutation, that have shorter circadian periods.

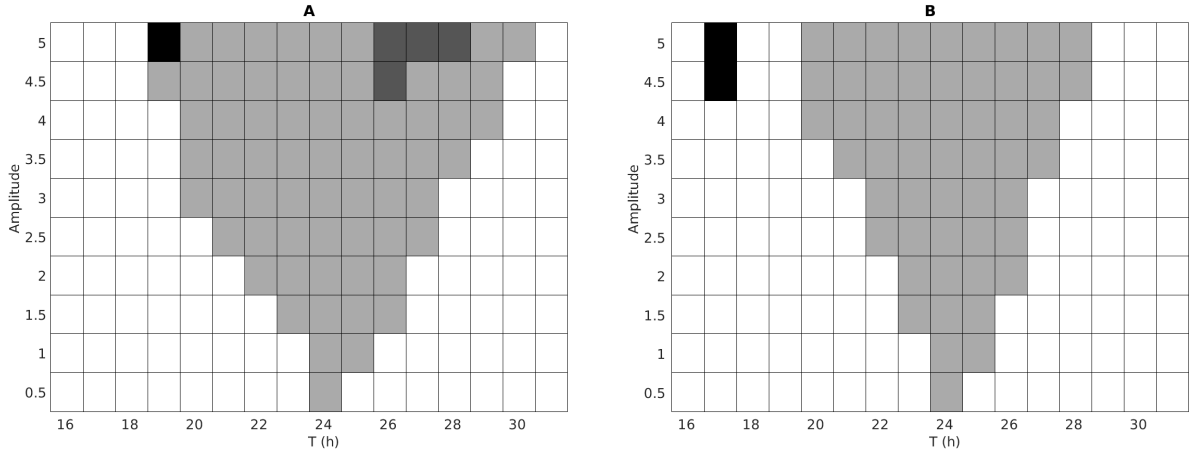


**Figure 7: Entrainment of the clock to an external oscillatory input.** The amplitude and the period of an entraining wave are varied and the resulting regions of entrainment form Arnold tongues. A) The entraining wave is a sinusoid. B) Entrainment is done with a rectangular wave. A black/white gradient represents the ratio between the clock period and the period of the entraining wave: white - no entrainment, grey - 1:1 entrainment, dark grey - 2:1 entrainment and black - 3:1 entrainment.

This mutation of the enzyme casein kinase  $1\epsilon$  ( $CK1\epsilon$ ) is thought to result in a gain of function on certain PER residues leading to its accelerated degradation, which is at the basis of the reduced period (Gallego et al., 2006) (Meng et al., 2008).

In this model, increasing  $\gamma_p$  leads to a shortening of the circadian period. This effect was shown in Fig. 12 and is also observed in the controlled model with chromatin remodeling here used (see Fig. 14). Though animals affected by the *tau* mutation have a shorter behavioral day, the underlying mechanism is a shortening of the molecular night, caused by accelerated degradation of PER after its peak expression (Meng et al., 2008). Here, we vary  $\gamma_p$  in a linear manner. An increase in  $\gamma_p$  corresponds to a gain of function of ( $CK1\epsilon$ ) and a decrease in  $\gamma_p$  to a loss of function of ( $CK1\epsilon$ ). This allows to investigate asymmetries in the clock's response to a decrease in period caused by increased PER degradation rate.

We start by measuring average durations of peak protein expression by computing the full width at half maximum (FWHM) as the length between the two instances at which the solution crosses half peak height:

$$FWHM = t_{down} - t_{up}, \quad \text{where } x(t_{up}) = x(t_{down}) = \frac{1}{2} x(t_{peak}), \quad t_{up} < t_{peak} < t_{down}$$

and  $t_{peak}$  is the instant at which the solution  $x(t)$  is at its maximum.

Fig. 8 shows the FWHM of all clock proteins, plotted against  $\gamma_p$ . Two vertical lines show the points where the period of the system is consistent with the wild type (WT) phenotype and with homozygotic  $CK1^{tau/tau}$  mutation to allow for better comparison. We observe that, the FWHM of proteins such as REV and PER decreases linearly with  $\gamma_p$  and the FWHM of PER:CRY also shows a decreasing trend for higher  $\gamma_p$  values, meaning that as the period decreases the duration of expression of these proteins also decreases. On the other hand, duration of expression of BMAL1 and CRY1 doesn't decrease linearly with the period and changes very little from the wild type to the *tau* mutation. This suggests an ability of the clock circuit to protect the duration of one of its main antiphasic molecular states (BMAL1, CRY1) against changes that affect the other (PER, PER:CRY), see Fig. 2.

Moreover, a measurement of the total amount of time spent at a particular molecular phase  $T_{total}$  in a given time window  $T_{window}$  can be given by the number of periods the system goes through in the time window  $\frac{T_{window}}{T}$  multiplied by the FWHM of the specific protein. Thus, we compute the ratio of total time spent at different molecular phases between  $CK1^{tau/tau}$  and  $CK1^{WT}$  as:

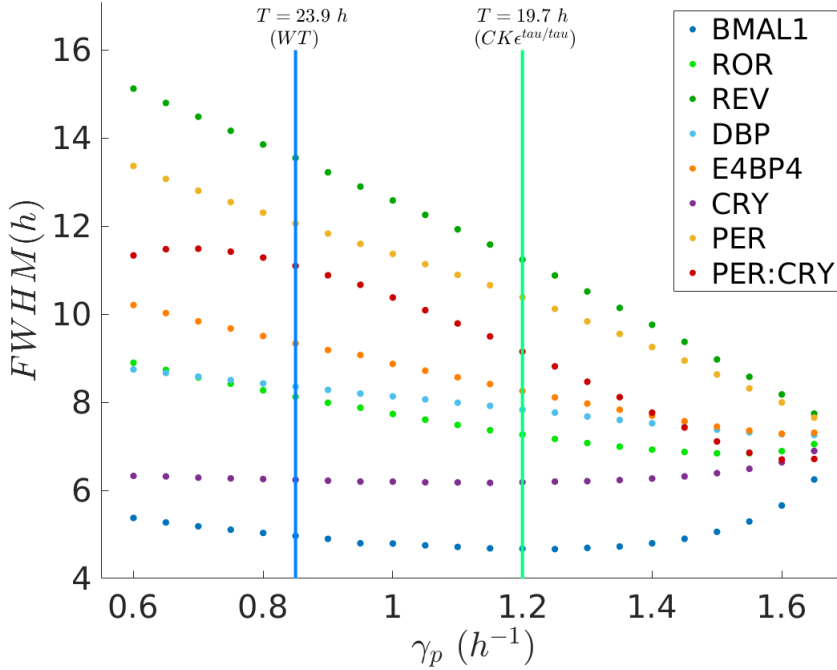


**Figure 8: Asymmetric changes of FWHM of several clock proteins as  $\gamma_p$  is varied.** When the period of the system is varied in a manner consistent with the  $\tau$  mutation the duration of protein expression decreases as the circadian period decreases (increase of  $\gamma_p$ ) for the majority of clock proteins, except for CRY1 and BMAL1. Vertical lines show the points where the period of the system is consistent with both the wild type phenotype and the  $\tau$  mutation.

$$\frac{T_{total}^{\tau} BMAL1}{T_{total}^{WT} BMAL1} = \frac{\frac{T_{window}}{T_{\tau}} FWHM_{BMAL1}^{\tau}}{\frac{T_{window}}{T_{WT}} FWHM_{BMAL1}^{WT}} = \frac{T_{WT} FWHM_{BMAL1}^{\tau}}{T_{\tau} FWHM_{BMAL1}^{WT}} = 1.14$$

and similarly

$$\frac{T_{total}^{\tau} CRY1}{T_{total}^{WT} CRY1} = 1.20, \quad \frac{T_{total}^{\tau} PER}{T_{total}^{WT} PER} = 1.05, \quad \frac{T_{total}^{\tau} PER:CRY}{T_{total}^{WT} PER:CRY} = 1.00$$

This means that in the same time window (which means comparing  $\tau$  and wild type mice with the same age) the  $\tau$  phenotype spends 14 % more time with elevated BMAL1 expression and 20 % more time with elevated CRY1 than the wild-type phenotype while spending about the same time in a state of elevated PER and PER:CRY expression. This is because while FWHM of PER and PER:CRY decreases with the decrease in period (Fig. 8), FWHM of CRY and BMAL1 changes little. Thus, the mutant with a shorter period results in more time spent at the BMAL1/CRY1 molecular state than the wild-type for a fixed time window.

The existence of two markedly distinct phases of response to  $\gamma_p$  may be implicated in metabolic processes and states, such as insulin sensitivity/resistance, that oscillate with the states of sleep and alertness: a state of feeding/alertness tends to be also of increased insulin sensitivity so as to allow cells to uptake glucose, in particular at the beginning of the activity phase (la Fleur et al., 2001). The  $\tau$  phenotype is characterized by a cluster of altered features that includes altered rates of growth and reproduction, body size and lifespan. Furthermore, metabolic rate relative to body mass is observed to increase proportionally to the increase in circadian frequency (Oklejewicz et al., 1997). Whether these phenomena are caused by pleiotropic effects of  $CK1\epsilon$  kinase or by the altered circadian rhythm is still a matter

of discussion. In fact, mammalian clock proteins not only control the formation of rate-limiting enzymes of several metabolic processes, but are also themselves directly involved in metabolism (Zhou et al., 2014) (Zhang et al., 2010).

Furthermore, our results reveal an ability of the clock circuit to protect the duration of one of its molecular phases (BMAL1, CRY1) against changes that affect the other (PER, PER:CRY) (see Fig. 2). For this, the dynamical clock mechanism behind two distinct circadian phases (BMAL1/PER:CRY) modeled in this work may be relevant. Fig. 15 shows an extended simulation of FWHM for BMAL1 and PER:CRY in a wider range of  $\gamma_p$ , where an opposite trend in variation between the FWHM of BMAL1 and of PER:CRY is visible.

Moreover, Fig. 16 shows that amplitude and mean value of BMAL1 and PER:CRY similarly decrease with  $\gamma_p$ . This decrease in amplitude may not be large enough to impair biological processes. In fact, observations show that the *tau* mutation doesn't significantly affect clock amplitude (Meng et al., 2008). Divergence with observations in this aspect may be due to our simplistic modeling. Importantly, in Fig. 16 the amplitude and mean value of BMAL1 and PER:CRY have similar trends of change with  $\gamma_p$ . Thus, the asymmetric response of the clock system to variations of  $\gamma_p$  concerns only the time spent at main clock phases, for which we focus mostly on the changes in BMAL1 and PER:CRY duration of expression and how these may relate to different metabolic states.

Additionally, Fig. 17 shows FWHM as percentage of circadian period for the same simulation as Fig. 8. Note the increase in the percentage of circadian period BMAL1 and CRY1 occupy versus other clock proteins.

To further this analysis, we observe the phase differences between peaks of BMAL1 and PER:CRY with  $\gamma_p$ . Assuming a cycle starts with BMAL1 increase, these phase differences reflect respectively the time difference between peaks of PER:CRY and previous BMAL1 peaks of the same cycle  $n$  and peaks of BMAL1 and the peaks of PER:CRY of the previous cycle, as:

$$\Delta\Phi_{[BMAL1,PER:CRY]} = t_{peaks_n}^{PER:CRY} - t_{peaks_n}^{BMAL1}$$

and

$$\Delta\Phi_{[PER:CRY,BMAL1]} = t_{peaks_n}^{BMAL1} - t_{peaks_{n-1}}^{PER:CRY}$$

Fig. 9 shows how the two half periods vary with  $\gamma_p$ . While  $\Delta\Phi_{[PER:CRY,BMAL1]}$  doesn't change  $\Delta\Phi_{[BMAL1,PER:CRY]}$  decreases linearly with  $\gamma_p$ , i.e. the shortening of the period is due to the PER:CRY peak occurring closer to the previous BMAL1 peak. Thus, the phase differences between BMAL1 and PER:CRY are also two possible useful measurements to investigate asymmetric effects in clock dynamics due to  $\gamma_p$ -dependent period changes. As such, when comparing the total time spent at each of these two molecular phases for *tau* and wild-type in the same time window we obtain:

$$\frac{T_{\Delta\Phi_{[PER:CRY,BMAL1]}^{tau}}}{T_{\Delta\Phi_{[PER:CRY,BMAL1]}^{WT}}} = \frac{T_{WT}\Delta\Phi_{[PER:CRY,BMAL1]}^{tau}}{T_{tau}\Delta\Phi_{[PER:CRY,BMAL1]}^{WT}} = 1.20$$

and

$$\frac{T_{\Delta\Phi_{[BMAL1,PER:CRY]}^{tau}}}{T_{\Delta\Phi_{[BMAL1,PER:CRY]}^{WT}}} = \frac{T_{WT}\Delta\Phi_{[BMAL1,PER:CRY]}^{tau}}{T_{tau}\Delta\Phi_{[BMAL1,PER:CRY]}^{WT}} = 0.90$$

i.e. the *tau* phenotype spends 20 % more time at the [PER:CRY, BMAL1] molecular state and 10 % less time at the [BMAL1, PER:CRY] molecular state than the wild-type.

Moreover, an example of two oscillatory solutions for the  $CKe^{WT}$  and  $CKe^{tau/tau}$  cases is shown in Fig. 18, where the phase differences and FWHM variation of both proteins between the two  $\gamma_p$  values can be seen. The FWHM of PER:CRY decreases more than the FWHM of BMAL1. Similarly, the shortening of the period affects more the  $\Delta\Phi_{[BMAL1,PER:CRY]}$  phase than the  $\Delta\Phi_{[PER:CRY,BMAL1]}$  phase, with the peaks of PER:CRY getting closer in time to the previous BMAL1 peaks, while the phase difference between BMAL1 peaks and previous PER:CRY peaks is maintained.

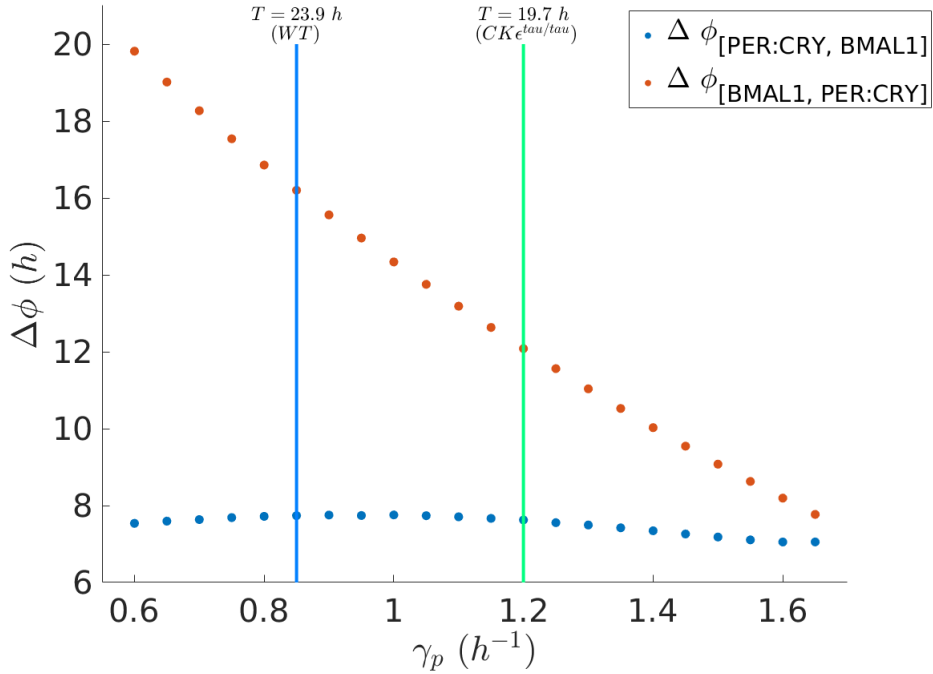


**Figure 9: Changes of  $\Delta\Phi_{[BMAL1,PER:CRY]}$  and  $\Delta\Phi_{[PER:CRY, BMAL1]}$  with the *tau* mutation.** As  $\gamma_p$  increases  $\Delta\Phi_{[PER:CRY, BMAL1]}$  remains approximately constant while  $\Delta\Phi_{[BMAL1, PER:CRY]}$  decreases linearly, i.e. the shortening of period that occurs with  $\gamma_p$  is compatible with asymmetric changes of the molecular clock phases. Vertical lines show the points where the period of the system is consistent with the wild type phenotype and with the *tau* mutation.

These results suggest there may be a role of the circadian clock in optimizing the time spent at each molecular phase. Hence, the relative duration of different clock phases, given either by the FWHM of each protein or by the phase difference between the peaks of proteins, may be relevant in the investigation of metabolic diseases.

A similar reasoning could be made for other cyclic processes that may have a circadian control. For example, a circadian rhythm of redox has been observed in the SCN (Wang et al., 2012) and a BMAL1-dependent circadian rhythm of ROS (reactive oxidative species) in mice fibroblasts (Khapre et al., 2011). Thus, assuming a circadian rhythm of redox in peripheral cells, we could relate the time spent at a specific stage of the cellular redox cycle with observations of altered lifespan. Importantly, *tau* mutant Syrian hamsters are observed to live 14 to 16 % longer than wild type (Oklejewicz and Daan, 2002). According to our results, the higher percentage of time spent with increased BMAL1 and/or CRY1 expression would be relevant for this phenomenon, as leading to decreased time spent at the oxidative state. This idea may be supported by the increased sensitivity of *Bmal1*<sup>-/-</sup> cells to oxidative stress and the premature aging of BMAL1-deficient mice (Khapre et al., 2011).

## 6. Clock integration of hormonal signaling and circadian alignment

To expand and deepen the relationship between the duration of the different circadian phases and metabolism, we investigate the role of the mammalian clock mechanism in integrating hormonal signaling.

A subject of interest is the response of the system to aligned and misaligned states between suprachiasmatic nucleus (SCN)-driven circadian light sensing and food/activity-related signaling. Circadian misalignment between the sleep/feeding schedule of individuals and the external light environment (occurring, for instance, in shift-workers) is known to increase the risk of several metabolic diseases such as diabetes, obesity, dyslipidemia, and insulin resistance which are all manifestations of metabolic syndrome (Brum et al., 2015) (Leproult et al., 2014).

Peripheral clocks are incapable of directly sensing light inputs. Nevertheless, light-induced SCN-driven hormonal

signaling is likely to be relevant for metabolic homeostasis in the entire organism, as phase misalignment between the internal clock and the external light environment decreases metabolic efficiency (West et al., 2017). (Ishida et al., 2005) demonstrate that the SCN of mice gates external light signals inducing phase-dependent corticosterone release by the adrenal gland via the sympathetic nervous system. Furthermore, this effect is proportional to the light intensity and indicates that external environmental light signals instantly provoke adrenal glucocorticoid release in the blood (Ishida et al., 2005).

Thus, adrenal production of glucocorticoids (GCs) is coordinated by the central nervous system and can be either humoral, via activation of the hypothalamic pituitary adrenal (HPA) axis as provoked by stress and fasting, or nervous via activation of the SCN-sympathetic nervous system by light (Ishida et al., 2005). GCs in turn act on peripheral cells via activation of the glucocorticoid receptor GR and are known to regulate the circadian clock and to cause an increase in PER expression. In general, a high GC state also correlates with the fasting state, but unlike insulin or glucagon that are exclusively dependent on nutrient status, GC plasma levels in mice can be induced by light, making it the hormonal signal of choice to represent indirect sensing of the light/dark cycle in peripheral molecular clocks. In fact, in aligned nocturnal animals, the fasting phase corresponds to the light window of the daily circadian cycle.

As such, to represent the light-dependent GR cycle we add an input in the equation of PER, Eq. (10), as done above for the entrainment study, which is a sinusoidal wave with a 24 h period (the same as the intrinsic period of the system), as *Per* genes have been shown to be the ultimate transcriptional targets of glucocorticoid signaling (So et al., 2009). On the other hand, the hormonal signal that better represents a feeding cycle is insulin. Insulin is known to trigger BMAL1 exclusion from the nucleus, suppressing its promoter activity (Dang et al., 2016). Thus, we introduce the degradation term:  $-insulin(t) [BMAL1]$  in Eq. (4), where *insulin*(*t*) is also sinusoidal wave with period  $T = 24$  h, meaning that a gradual change occurs between a feeding (activity) and a fasting (rest) phase (of 12 hours each). We keep the two signals with the same amplitude  $A = 1$  and period  $T = 24$  h and vary only the phase between them, as in  $GR(t) = A + A \cos(\frac{2\pi}{T}t)$  and  $insulin(t) = A + A \cos(\frac{2\pi}{T}(t + \Delta\phi))$ , where  $\Delta\phi$  is the phase difference between the two signals in hours. We compute the FWHM of all clock proteins in response to  $\Delta\phi$  (varying between 0 and 24 h). As our model was built on and calibrated to data of nocturnal animals (mice and rats) (Feillet et al., 2014) (Ueda et al., 2005), we consider the aligned state to be represented by  $\Delta\phi \approx 12$  h.

In Fig. 10 we observe how the FWHM of each clock protein changes as the phase difference  $\Delta\phi$  between the two signals varies from 0 to 24 hours. Strikingly, duration of BMAL1 and PER:CRY peak expression has opposite trends in change, meaning that  $\Delta\phi$  affects the time spent at each of these two main circadian clock phases. This can possibly result in different time spent at different metabolic states or processes, as well as in alteration of the quantities of metabolic enzymes for which clock proteins are rate-limiting. Duration of BMAL1 peak expression has a maximum when the signals are in phase opposition (circadian alignment) and a minimum when the signals are in phase (circadian misalignment), with FWHM of CRY, ROR and E4BP4 also increasing when signals move out of phase. On the other hand, REV and PER:CRY seem to have a maximum for signals in phase. Curiously, average duration of PER peak expression seems to be constant. In all simulations the order of peak expression of clock proteins was unaltered, and the same as in Fig. 2.

These simulations show dynamic variations in the core clock components due to changes in regulatory inputs. An interpretation of these results can be provided in the light of the pervasive involvement of the circadian clock in metabolism and noticing that circadian misalignment has been shown to promote insulin resistance independently of sleep loss (Leproult et al., 2014) (Reinke and Asher, 2019). Considering the role of BMAL1 in promoting insulin sensitivity in mouse liver and muscle (Zhou et al., 2014) (Dyar et al., 2014), as well as the fact that CRY1, here presenting a similar trend as BMAL1, also plays a role in improving hepatic insulin sensitivity (Zhang et al., 2010), these results may help to explain the higher incidence of insulin resistance in individuals subjected to circadian misalignment: as duration of circadian phases varies and the percentage of circadian period with higher BMAL1 and CRY1 expression decreases so does the time spent in (directly or indirectly) promoting processes of insulin sensitivity.

Though light is a known stressor in mice that are nocturnal prey animals, GCs are released in all mammals at the end of the resting phase and the neuroanatomy connecting the brain to the adrenals is similar in mice and humans. Furthermore, a similar type of signaling is conceivable in a variety of organisms and the impact of misalignment in generating changes in the duration of the different clock phases may be relevant for different systems. Expanding these ideas for humans would require a confirmation of the number and combinations of boxes at gene promoters sufficient for antiphase CLOCK:BMAL1/PER:CRY oscillation as well as calibration from human data. Nevertheless, the fact that this is a mammalian model strengthens the hypothesis that an asymmetric change in the duration of different circadian molecular phases might be a consequence of misalignment for humans as well. Experimental observations

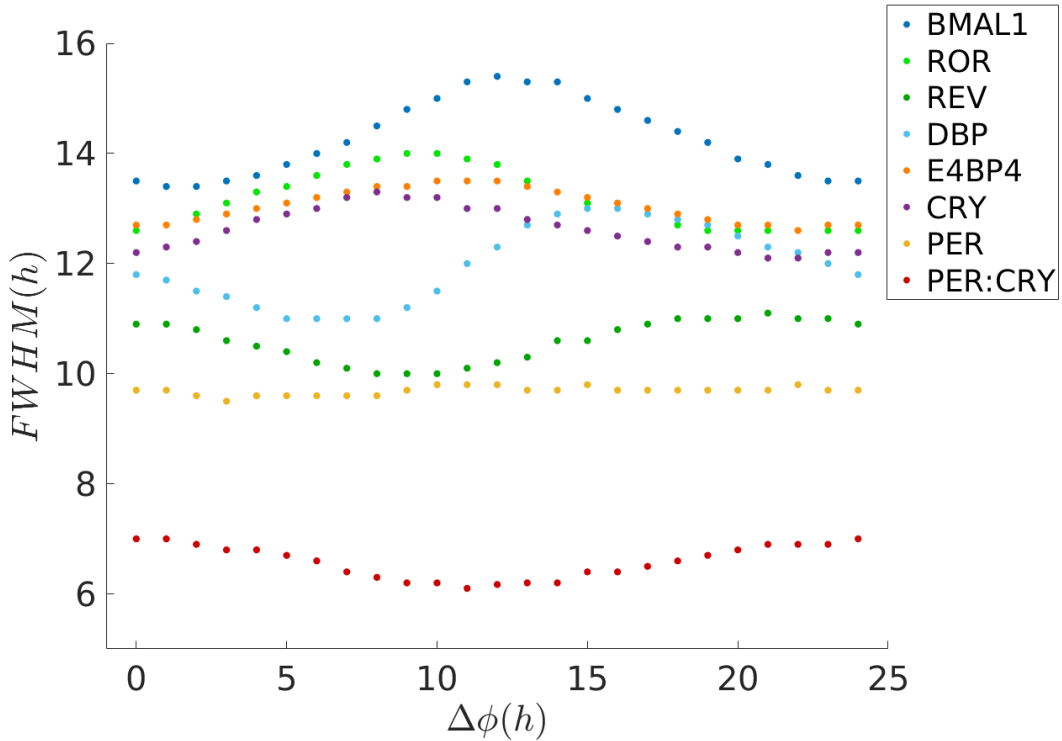


**Figure 10: Variations of FWHM with the phase difference between two external hormonal signals.** Changes in FWHM, as the phase difference between two crossed regulatory inputs changes. Duration of BMAL1, ROR, CRY1 and E4BP4 expression increases when the signals move out of phase, while duration of REV and PER:CRY decreases. FWHM of PER changes little with  $\Delta\phi$ .

both in mice and in humans of changes in FWHM in response to food/light misalignment would allow to evaluate our hypothesis. Overall, Fig. 10 gives predictions of the response of the mammalian clock to the phase relation between any two input signals (one acting via promoting PER and other via BMAL1 removal from target promoters) and shows that different states of alignment/misalignment between this signals result in different percentages of time spent at different clock phases and processes.

The analysis presented in this Section pieces together information on the mammalian clock, namely that misalignment with the light environment is observed to decrease metabolic efficiency (West et al., 2017) and that light activates adrenal release of GCs (Ishida et al., 2005). Furthermore, a feeding-dependent 24 h insulin cycle is here proposed to be a decisive factor in determining the aligned/misaligned state. This allowed to construct an idea of what type of signals could be acting on peripheral clocks and how. Our approach is simplistic as, realistically, there are several simultaneous ways by which the clock might incorporate metabolic signals, as well as more regulatory loops. Importantly, CLOCK:BMAL1 affects insulin production in pancreatic  $\beta$  cells (Perelis et al., 2015). Here, we assume there are no restrictions in insulin production to study its effects in peripheral clocks, i.e. insulin is produced any time feeding occurs and peripheral cells receive a sinusoidal wave of insulin over 24 h. As such, the work here developed could be expanded to include more regulatory loops and signals. A recent example of a comprehensive clock/metabolism model that includes pancreatic insulin production is that of (Woller and Gonze, 2018) that observe gene-specific phase shifts in result to misalignment between light and food cues. Nevertheless, our simplistic approach has the advantage of allowing to better study isolated effects of each signal.

Moreover, the modeling here developed suggests a mechanism for the observed control of the glucose tolerance cycle by the SCN (la Fleur et al., 2001). Similarly, our results concerning the FWHM response to one food-related and one SCN-dependent signal led us to hypothesize a way whereby the 24 h insulin sensitivity cycle can be affected by peripheral clocks.

The currently accepted view states that circadian misalignment causes metabolic disease by desynchronizing the clocks of different internal organs and systems. Our hypothesis aims to provide a new, possibly complementary, insight whereby circadian misalignment can change the relative duration of activating and repressing molecular clock states of internal clocks and consequently promote a smaller percentage of time spent in processes that favor insulin sensitivity, thus leading to altered metabolic markers. As mentioned above, this interpretation could be extended for other processes of potential circadian control, such as cellular redox that connects with lifespan. On this regard, a decrease in lifespan is observed for chronic circadian misalignment in *Drosophila* (Boomgarden et al., 2019).

The circadian clock is thus here interpreted as a system that receives signaling inputs and outputs time spent at different cellular processes.

## 7. Conclusion

Our analysis illustrates a description of the circadian clock mechanism by a network of regulations occurring mostly at the transcription level. This is due to the ability of circadian genes to transduce a variety of signals, as well as to the whole architecture of the system that is able to sense and integrate external and internal inputs, with likely implications in a variety of cellular processes, including metabolic processes. In this perspective, we developed a transcription-based dynamic model, with standard mathematical formalism and a reduced number of equations and parameters, that is indeed capable of reproducing the relative order of expression of the main clock proteins, with special emphasis on the antiphasic relation between BMAL1 and PER:CRY that relate to opposite phases of the fast/feeding, rest/activity cycles. The modeling framework here developed is a tool that can be used for dynamic modeling of genetic networks of this type, and consists generally in describing protein rates of change as a combination of independent responses to certain regions of the genome, that in this case are the CCEs: E-box, R-box and D-box. Changes at these regions of the genome in turn are modeled by the competition between activators and repressors.

Investigations on changes of the PER degradation rate, compatible with the *tau* mutation mechanism, have shown the average duration of peak expression to decrease with the frequency for the majority of clock proteins, but not for BMAL1 and CRY1. Moreover, when one signal representative of the light/dark cycle and another signal representing the fast/feeding cycle are simultaneously applied, the peak duration of BMAL1 is maximal when the feeding behavior occurs at a correct time and minimal when the feeding behavior occurs the most out of its expected phase; an opposite effect is observed for PER:CRY. As we may directly connect BMAL1 with increased insulin sensitivity, these observations help to connect the state of insulin resistance with altered time pattern of feeding behavior that is observed for shift-workers and in people affected by metabolic syndrome (Brum et al., 2015), leading us to propose that the control of molecular state duration may be an important mechanism of the clock relevant for its connection with metabolic homeostasis.

## Acknowledgments

The authors are part of the Labex SIGNALIFE Network for Innovation on signal Transduction Pathways in Life Sciences (Grant ANR-11-LABX-0028-01) and ICycle project (ANR-16-CE33-0016-01).

## References

- Becker-Weimann, S., Wolf, J., Herzel, H., Kramer, A., 2004. Modeling feedback loops of the mammalian circadian oscillator. *Biophysical journal* 87, 3023–34.
- Bell-Pedersen, D., Cassone, V.M., Earnest, D.J., Golden, S.S., Hardin, P.E., Thomas, T.L., Zoran, M.J., 2005. Circadian rhythms from multiple oscillators: lessons from diverse organisms. *Nature Reviews Genetics* 6, 544.
- Bieler, J., Cannavo, R., Gustafson, K., Gobet, C., Gatfield, D., Naef, F., 2014. Robust synchronization of coupled circadian and cell cycle oscillators in single mammalian cells. *Mol Syst Biol.* 15, 739.
- Boomgarden, A.C., Sagewalker, G.D., Shah, A.C., Haider, S.D., Patel, P., Wheeler, H.E., Dubowy, C.M., Cavanaugh, D.J., 2019. Chronic circadian misalignment results in reduced longevity and large-scale changes in gene expression in *drosophila*. *BMC genomics* 20, 14.
- Boulos, Z., Macchi, M.M., Terman, M., 2002. Twilights widen the range of photic entrainment in hamsters. *Journal of biological rhythms* 17, 353–363.
- Brum, M.C.B., Filho, F.F.D., Schnorr, C.C., Bottega, G.B., Rodrigues, T.C., 2015. Shift work and its association with metabolic disorders. *Diabetology & Metabolic Syndrome* 7, 45. doi:10.1186/s13098-015-0041-4.
- Buhr, E.D., Takahashi, J.S., 2013. Molecular components of the mammalian circadian clock, in: *Circadian clocks*. Springer, pp. 3–27.
- Crumbley, C., Wang, Y., Kojetin, D.J., Burris, T.P., 2010. Characterization of the core mammalian clock component, *nps2*, as a *rev-erbalpha/roalpha* target gene. *The Journal of biological chemistry* 285, 35386–92. doi:10.1074/jbc.M110.129288.

- Dang, F., Sun, X., Ma, X., Wu, R., Zhang, D., Chen, Y., Xu, Q., Wu, Y., Liu, Y., 2016. Insulin post-transcriptionally modulates bmal1 protein to affect the hepatic circadian clock. *Nature communications* 7, 12696.
- Dyar, K.A., Ciciliot, S., Wright, L.E., Biensø, R.S., Tagliazucchi, G.M., Patel, V.R., Forcato, M., Paz, M.I., Gudiksen, A., Solagna, F., et al., 2014. Muscle insulin sensitivity and glucose metabolism are controlled by the intrinsic muscle clock. *Molecular metabolism* 3, 29–41.
- Everett, L.J., Lazar, M.A., 2014. Nuclear receptor rev-erb- $\alpha$ : Up, down, and all around. *Trends Endocrinol Metab.* 1 25, 586–592. doi:10.1016/j.tem.2014.06.011.
- Feillet, C., van der Horst, G.T.J., Levi, F., Rand, D.A., Delaunay, F., 2015. Coupling between the circadian clock and cell cycle oscillators: Implication for healthy cells and malignant growth. *Frontiers in Neurology* 6, 96. doi:10.3389/fneur.2015.00096.
- Feillet, C., Krusche, P., Tamanini, F., Janssens, R.C., Downey, M.J., Martin, P., Teboul, M., Saito, S., Lévi, F.A., Bretschneider, T., van der Horst, G.T.J., Delaunay, F., Rand, D.A., 2014. Phase locking and multiple oscillating attractors for the coupled mammalian clock and cell cycle. *Proceedings of the National Academy of Sciences of the United States of America* 111, 9828–33. doi:10.1073/pnas.1320474111.
- la Fleur, S.E., Kalsbeek, A., Wortel, J., Fekkes, M.L., Buijs, R.M., 2001. A daily rhythm in glucose tolerance: a role for the suprachiasmatic nucleus. *Diabetes* 50, 1237–43.
- Forger, D.B., Peskin, C.S., 2003. A detailed predictive model of the mammalian circadian clock. *Proc Natl Acad Sci U S A* 100, 14806–11.
- Gallego, M., Eide, E.J., Woolf, M.F., Virshup, D.M., Forger, D.B., 2006. An opposite role for tau in circadian rhythms revealed by mathematical modeling. *Proceedings of the National Academy of Sciences of the United States of America* 103, 10618–23.
- Gallego, M., Virshup, D.M., 2007. Post-translational modifications regulate the ticking of the circadian clock. *Nature reviews. Molecular cell biology* 8, 139–48.
- Gérard, C., Goldbeter, A., 2012. Entrainment of the mammalian cell cycle by the circadian clock: modeling two coupled cellular rhythms. *PLoS computational biology* 8, e1002516. doi:10.1371/journal.pcbi.1002516.
- Gonze, D., Goldbeter, A., 2000. Entrainment versus chaos in a model for a circadian oscillator driven by light-dark cycles. *Journal of Statistical Physics* 101, 649–663.
- Goodwin, B.C., 1965. Oscillatory behavior in enzymatic control processes. *Advances in enzyme regulation* 3, 425–437.
- Heiland, I., Bodenstein, C., Hinze, T., Weisheit, O., Ebenhoeh, O., Mittag, M., Schuster, S., 2012. Modeling temperature entrainment of circadian clocks using the arrhenius equation and a reconstructed model from chlamydomonas reinhardtii. *Journal of biological physics* 38, 449–464.
- Ishida, A., Mutoh, T., Ueyama, T., Bando, H., Masubuchi, S., Nakahara, D., Tsujimoto, G., Okamura, H., 2005. Light activates the adrenal gland: timing of gene expression and glucocorticoid release. *Cell metabolism* 2, 297–307.
- Jolley, C., Ukai-Tadenuma, M., Perrin, D., Ueda, H., 2014. A mammalian circadian clock model incorporating daytime expression elements. *Biophys J.* 107, 1462–1473.
- Khapre, R.V., Kondratova, A.A., Susova, O., Kondratov, R.V., 2011. Circadian clock protein bmal1 regulates cellular senescence in vivo. *Cell cycle* 10, 4162–4169.
- Ko, C.H., Takahashi, J.S., 2006. Molecular components of the mammalian circadian clock. *Human molecular genetics* 15, R271–R277.
- Koike, N., Yoo, S.H., Huang, H.C., Kumar, V., Lee, C., Kim, T.K., Takahashi, J.S., 2012. Transcriptional architecture and chromatin landscape of the core circadian clock in mammals. *Science* 338, 349–354.
- Korenčič, A., Bordyugov, G., Košir, R., Rozman, D., Goličnik, M., Herzel, H., 2012. The interplay of cis-regulatory elements rules circadian rhythms in mouse liver. *PLoS one* 7, e46835. doi:10.1371/journal.pone.0046835.
- Lefta, M., Wolff, G., Esser, K.A., 2011. Circadian rhythms, the molecular clock, and skeletal muscle. *Current topics in developmental biology* 96, 231–71. doi:10.1016/B978-0-12-385940-2.00009-7.
- Leloup, J.C., Goldbeter, A., 2003. Toward a detailed computational model for the mammalian circadian clock. *Proceedings of the National Academy of Sciences of the United States of America* 100, 7051–6.
- Leproult, R., Holmbäck, U., Van Cauter, E., 2014. Circadian misalignment augments markers of insulin resistance and inflammation, independently of sleep loss. *Diabetes* 63, 1860–1869.
- Meng, Q.J., Logunova, L., Maywood, E.S., Gallego, M., Lebiecki, J., Brown, T.M., Sládek, M., Semikhodskii, A.S., Glossop, N.R., Piggins, H.D., et al., 2008. Setting clock speed in mammals: the ckl-epsilon tau mutation in mice accelerates circadian pacemakers by selectively destabilizing period proteins. *Neuron* 58, 78–88.
- Mirsky, H.P., Liu, A.C., Welsh, D.K., Kay, S.A., Doyle, F. J., r., 2009. A model of the cell-autonomous mammalian circadian clock. *Proc Natl Acad Sci U S A* 106, 11107–12.
- Oklejewicz, M., Daan, S., 2002. Enhanced longevity in tau mutant syrian hamsters, mesocricetus auratus. *Journal of biological rhythms* 17, 210–216.
- Oklejewicz, M., Hut, R.A., Daan, S., Loudon, A.S., Stirland, A.J., 1997. Metabolic rate changes proportionally to circadian frequency in tau mutant syrian hamsters. *Journal of biological rhythms* 12, 413–22.
- Pendegast, J.S., Friday, R.C., Yamazaki, S., 2010. Photic entrainment of period mutant mice is predicted from their phase response curves. *Journal of Neuroscience* 30, 12179–12184.
- Perelis, M., Marcheva, B., Ramsey, K.M., Schipma, M.J., Hutchison, A.L., Taguchi, A., Peek, C.B., Hong, H., Huang, W., Omura, C., et al., 2015. Pancreatic  $\beta$  cell ensembles regulate rhythmic transcription of genes controlling insulin secretion. *Science* 350, aac4250.
- Podkolodnaya, O.A., Tverdokhle, N.N., Podkolodny, N.L., 2017. Computational modeling of the cell-autonomous mammalian circadian oscillator. *BMC Systems Biology* 11, 27–42.
- Ramsey, K.M., Yoshino, J., Brace, C.S., Abrassart, D., Kobayashi, Y., Marcheva, B., Hong, H.K., Chong, J.L., Buhr, E.D., Lee, C., et al., 2009. Circadian clock feedback cycle through nampt-mediated nad<sup>+</sup> biosynthesis. *Science* 324, 651–654.
- Reddy, T.E., Gertz, J., Crawford, G.E., Garabedian, M.J., Myers, R.M., 2012. The hypersensitive glucocorticoid response specifically regulates period 1 and expression of circadian genes. *Molecular and cellular biology* 32, 3756–3767.
- Reinke, H., Asher, G., 2019. Crosstalk between metabolism and circadian clocks. *Nature Reviews Molecular Cell Biology* , 1.
- Relógio, A., Westermark, P.O., Wallach, T., Schellenberg, K., Kramer, A., Herzel, H., 2011. Tuning the mammalian circadian clock: robust synergy

- of two loops. *PLoS computational biology* 7, e1002309.
- Saini, C., Morf, J., Stratmann, M., Gos, P., Schibler, U., 2012. Simulated body temperature rhythms reveal the phase-shifting behavior and plasticity of mammalian circadian oscillators. *Genes & development* 26, 567–580.
- Smolen, P., Byrne, J., 2009. Circadian rhythm models, in: Squire, L.R. (Ed.), *Encyclopedia of Neuroscience*. Academic Press, Oxford, pp. 957–963. doi:<https://doi.org/10.1016/B978-008045046-9.01433-9>.
- So, A.Y.L., Bernal, T.U., Pillsbury, M.L., Yamamoto, K.R., Feldman, B.J., 2009. Glucocorticoid regulation of the circadian clock modulates glucose homeostasis. *Proceedings of the National Academy of Sciences* 106, 17582–17587.
- Tamaru, T., Hattori, M., Honda, K., Benjamin, I., Ozawa, T., Takamatsu, K., 2011. Synchronization of circadian *per2* rhythms and *hsf1-bmal1*: Clock interaction in mouse fibroblasts after short-term heat shock pulse. *PLoS one* 6, e24521.
- Tang, B.L., 2016. *Sirt1* and the mitochondria. *Molecules and cells* 39, 87.
- Trott, A.J., Menet, J.S., 2018. Regulation of circadian clock transcriptional output by clock: *Bmal1*. *PLoS genetics* 14, e1007156.
- Ueda, H.R., Hayashi, S., Chen, W., Sano, M., Machida, M., Shigeyoshi, Y., Iino, M., Hashimoto, S., 2005. System-level identification of transcriptional circuits underlying mammalian circadian clocks. *Nature genetics* 37, 187–92. doi:[10.1038/ng1504](https://doi.org/10.1038/ng1504).
- Ukai-Tadenuma, M., Yamada, R.G., Xu, H., Ripperger, J.A., Liu, A.C., Ueda, H.R., 2011. Delay in feedback repression by cryptochrome 1 is required for circadian clock function. *Cell* 144, 268–81. doi:[10.1016/j.cell.2010.12.019](https://doi.org/10.1016/j.cell.2010.12.019).
- Wang, T.A., Yanxun, V.Y., Govindaiah, G., Ye, X., Artinian, L., Coleman, T.P., Sweedler, J.V., Cox, C.L., Gillette, M.U., 2012. Circadian rhythm of redox state regulates excitability in suprachiasmatic nucleus neurons. *Science* 337, 839–842.
- West, A.C., Smith, L., Ray, D.W., Loudon, A.S., Brown, T.M., Bechtold, D.A., 2017. Misalignment with the external light environment drives metabolic and cardiac dysfunction. *Nature communications* 8, 417.
- Woller, A., Duez, H., Staels, B., Lefranc, M., 2016. A mathematical model of the liver circadian clock linking feeding and fasting cycles to clock function. *Cell Rep.* 17, 1087–1097.
- Woller, A., Gonze, D., 2018. Modeling clock-related metabolic syndrome due to conflicting light and food cues. *Sci Rep.* 8, 13641.
- Yamaguchi, S., Mitsui, S., Yan, L., Yagita, K., Miyake, S., Okamura, H., 2000. Role of *dbp* in the circadian oscillatory mechanism. *Molecular and cellular biology* 20, 4773–81.
- Yamamoto, T., Nakahata, Y., Soma, H., Akashi, M., Mamine, T., Takumi, T., 2004. Transcriptional oscillation of canonical clock genes in mouse peripheral tissues. *BMC molecular biology* 5, 18.
- Yan, J., Xu, Y., Yang, L., Shi, G., Xing, L., Wu, X., Dong, Z., Zhang, Z., Qu, Z., Liu, Z., 2014. An intensity ratio of interlocking loops determines circadian period length. *Nucleic Acids Research* 42, 10278–10287. doi:[10.1093/nar/gku701](https://doi.org/10.1093/nar/gku701).
- Yang, F., Inoue, I., Kumagai, M., Takahashi, S., Nakajima, Y., Ikeda, M., 2013. Real-time analysis of the circadian oscillation of the *rev-erb-beta* promoter. *Journal of atherosclerosis and thrombosis* 20, 267–76.
- Ye, R., Selby, C.P., Chiou, Y.Y., Ozkan-Dagliyan, I., Gaddameedhi, S., Sancar, A., 2014. Dual modes of clock: *Bmal1* inhibition mediated by cryptochrome and period proteins in the mammalian circadian clock. *Genes & development* 28, 1989–1998.
- Zámborszky, J., Hong, C.I., Csikász Nagy, A., 2007. Computational analysis of mammalian cell division gated by a circadian clock: quantized cell cycles and cell size control. *Journal of biological rhythms* 22, 542–53.
- Zamir, I., Zhang, J., Lazar, M.A., 1997. Stoichiometric and steric principles governing repression by nuclear hormone receptors. *Genes & development* 11, 835–46.
- Zehring, W.A., Wheeler, D.A., Reddy, P., Konopka, R.J., Kyriacou, C.P., Rosbash, M., Hall, J.C., 1984. P-element transformation with period locus *dna* restores rhythmicity to mutant, arrhythmic *drosophila melanogaster*. *Cell* 39, 369–376.
- Zhang, E.E., Liu, Y., Dentin, R., Pongsawakul, P.Y., Liu, A.C., Hirota, T., Nusinow, D.A., Sun, X., Landais, S., Kodama, Y., Brenner, D.A., Montminy, M., Kay, S.A., 2010. Cryptochrome mediates circadian regulation of camp signaling and hepatic gluconeogenesis. *Nature medicine* 16, 1152–6. doi:[10.1038/nm.2214](https://doi.org/10.1038/nm.2214).
- Zhou, B., Zhang, Y., Zhang, F., Xia, Y., Liu, J., Huang, R., Wang, Y., Hu, Y., Wu, J., Dai, C., Wang, H., Tu, Y., Peng, X., Wang, Y., Zhai, Q., 2014. Clock/*bmal1* regulates circadian change of mouse hepatic insulin sensitivity by *sirt1*. *Hepatology* (Baltimore, Md.) 59, 2196–206. doi:[10.1002/hep.26992](https://doi.org/10.1002/hep.26992).

## A. Supporting Material

Repressors	Activators	Targets	Response element (box)	Mechanism
REV-ERB $\alpha$ , REV-ERB $\beta$	ROR $\alpha$ , ROR $\beta$ , ROR $\gamma$	<i>Bmal1, Clock, Cry1, RORc, E4BP4</i>	R-box	Competition on DNA
PER1, PER2, PER3, CRY1, CRY2	CLOCK, BMAL1	<i>Per1, Per2, Per3, Cry1, Rev-erba Rev-erb<math>\beta</math>, RORc, Dbp</i>	E-box	Protein-protein interaction
E4BP4	DBP, HLF, TEF	<i>Per1, Per2, Per3, Rev-erba Rev-erb<math>\beta</math>, RORa, RORb,</i>	D-box	Competition on DNA

**Figure 11: Regulatory mechanisms of the three major CCEs.** RORs and REVs compete for R-box binding. CLOCK:BMAL1 acts as an E-box activator and CRYs or PER:CRYs can bind to a previously bound CLOCK:BMAL1 repressing its E-box promoter activity. D-box can be activated by DBP, HLF and TEF and repressed by E4BP4.

**Table 1**

Calibrated parameters from REV-ERB $\alpha$  data from (Feillet et al., 2014), (as shown in Fig.2), for the circadian clock model.

p	Numerical Value
$V_R$	44.4 $\%.h^{-1}$
$k_R$	3.54 %
$k_{Rr}$	80.1 %
$V_E$	30.3 $\%.h^{-1}$
$k_E$	214 %
$k_{Er}$	1.24 %
$V_D$	202 $\%.h^{-1}$
$k_D$	5.32 %
$k_{Dr}$	94.7 %
$\gamma_{ror}$	2.55 $h^{-1}$
$\gamma_{rev}$	0.241 $h^{-1}$
$\gamma_p$	0.844 $h^{-1}$
$\gamma_c$	2.34 $h^{-1}$
$\gamma_{db}$	0.156 $h^{-1}$
$\gamma_{E4}$	0.295 $h^{-1}$
$\gamma_{pc}$	0.191 $\%^{-1}.h$
$\gamma_{cp}$	0.141 $h^{-1}$
$\gamma_{bp}$	2.58 $\%^{-1}.h$

## Transcription-based circadian mechanism controls the duration

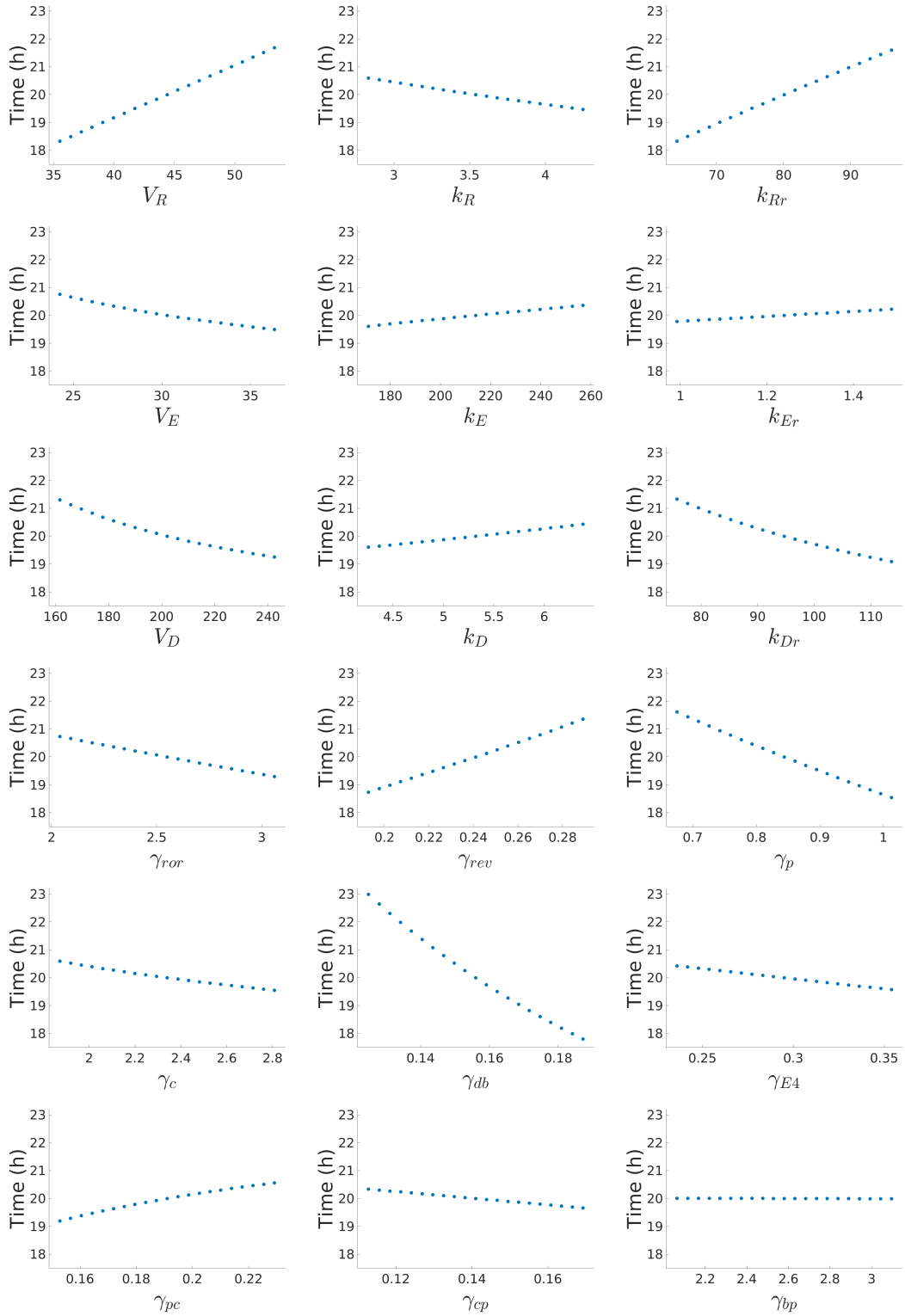


**Figure 12: Sensitivity analysis: the model is robust to the variation of parameters.** Each parameter is varied 20% around the calibrated point (Table 1) and oscillations are always present. Variations in the value of  $V_R$ ,  $k_R$ ,  $k_{Rr}$ ,  $\gamma_{ror}$ ,  $\gamma_{db}$  and  $\gamma_p$  significantly alter the period of the system, while varying  $k_E$ ,  $k_{Er}$ ,  $\gamma_{bp}$ ,  $\gamma_{E4}$  and  $k_D$  has little impact on the oscillatory period.

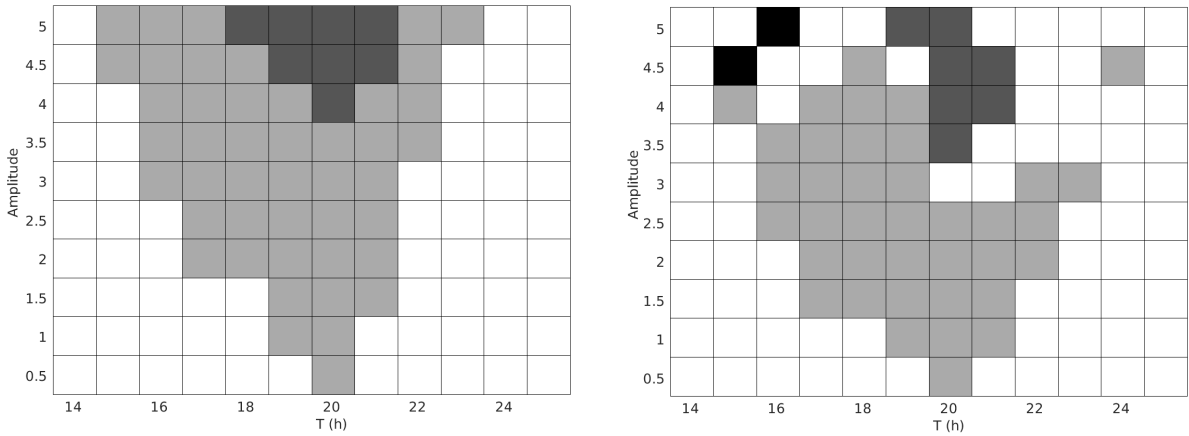


**Figure 13: Entrainment of the clock model without chromatin remodeling to an external oscillatory input.** The amplitude and the period of an entraining wave are varied and the resulting regions of entrainment form Arnold tongues. A) The entraining wave is a sinusoid. B) Entrainment is done with a rectangular wave. A black/white gradient represents the ratio between the clock period and the period of the entraining wave: white - no entrainment, grey - 1:1 entrainment, dark grey - 2:1 entrainment and black - 3:1 entrainment. By comparison with Fig. 7 incorporation of the chromatin remodeling mechanism results in a larger region of entrainment for sinusoidal waves and an improved entrainment overall for square waves.

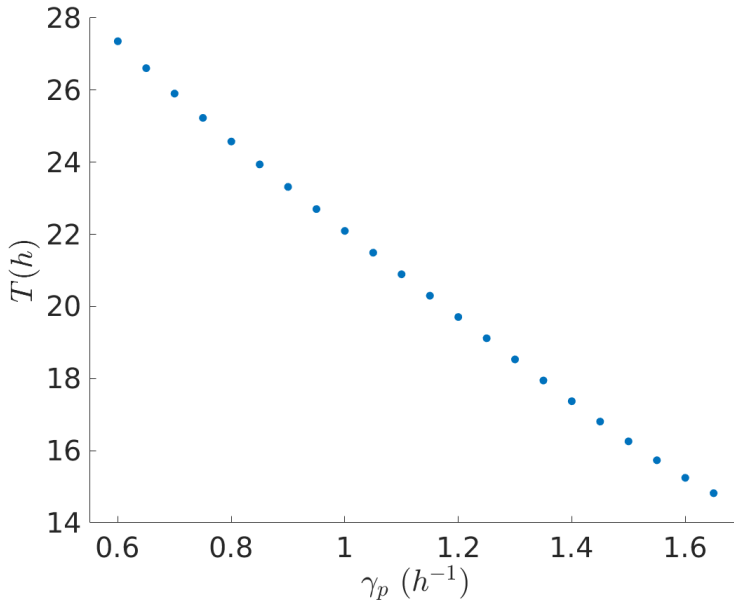


**Figure 14: Period changes with  $\gamma_p$ .** The period of the system with chromatin remodeling decreases linearly with  $\gamma_p$ .

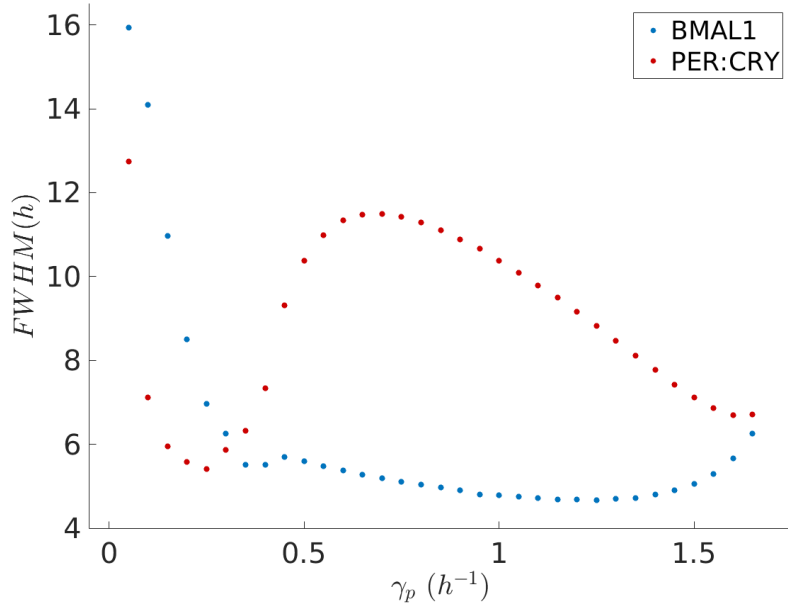


**Figure 15: FWHM of BMAL1 and PER:CRY for a wide range of  $\gamma_p$ .** FWHM of BMAL1 and PER:CRY tend to have opposite trends of change with  $\gamma_p$ .

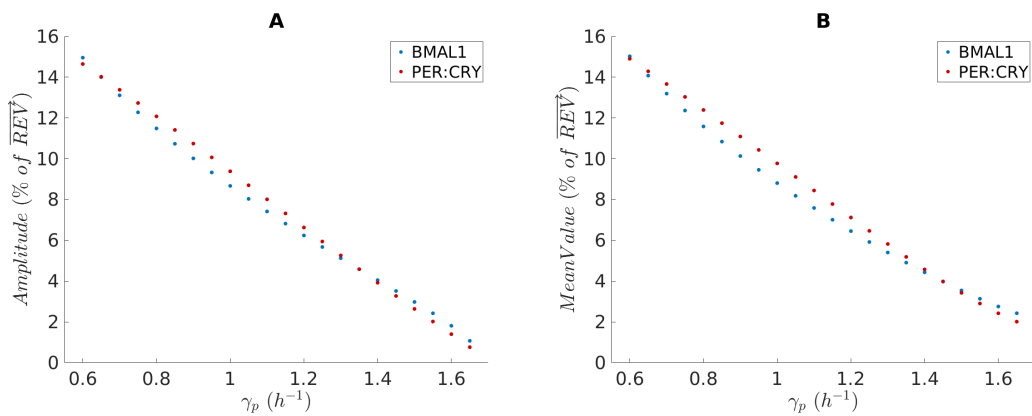


**Figure 16: Amplitude and mean value of BMAL1 and PER:CRY similarly decrease with  $\gamma_p$ .** The amplitude and mean value of BMAL1 and PER:CRY are similarly affected by changes in  $\gamma_p$ .

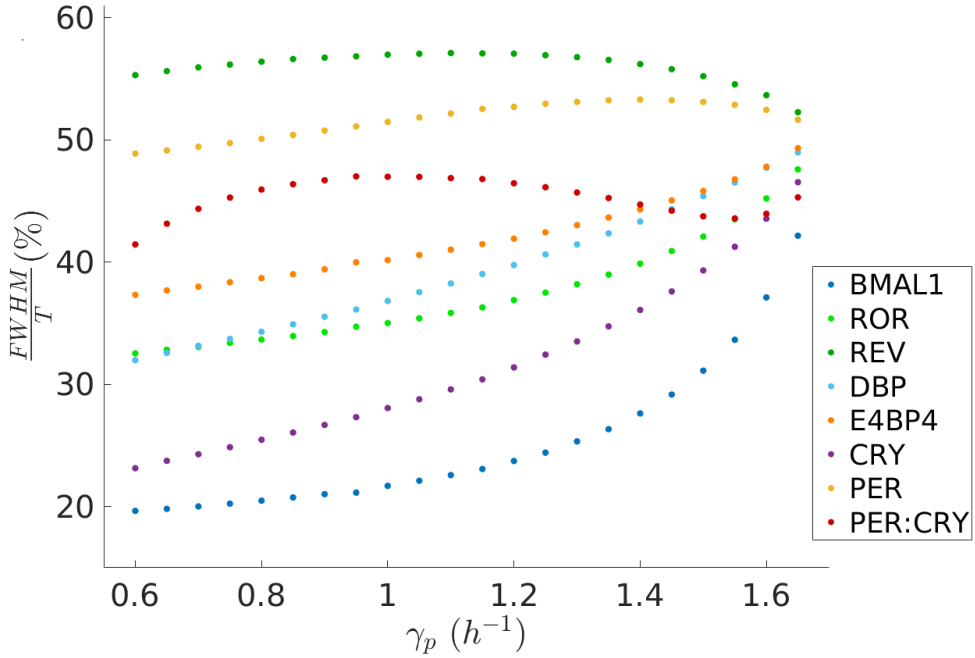


**Figure 17: Ratio of FWHM to circadian period  $T$  of each clock protein with  $\gamma_p$  (same simulation as Fig. 8).** The percentage of circadian period spent at the BMAL1 and CRY1 molecular phases increases with  $\gamma_p$ . By comparison, the FWHM per period of the remaining clock proteins varies less with  $\gamma_p$ , especially in the region of  $\gamma_p$  that comprises periods compatible with variations between  $CK\epsilon^{WT}$  and  $CK\epsilon^{\tau/\tau}$ , ( $0.85 \text{ h}^{-1} \leq \gamma_p \leq 1.2 \text{ h}^{-1}$ ). Note that the system's period also changes with  $\gamma_p$ . To compare the percentage of time spent at each molecular clock phase of two different  $\gamma_p$  values for a fixed time window refer to Fig. 8 and Section 5.

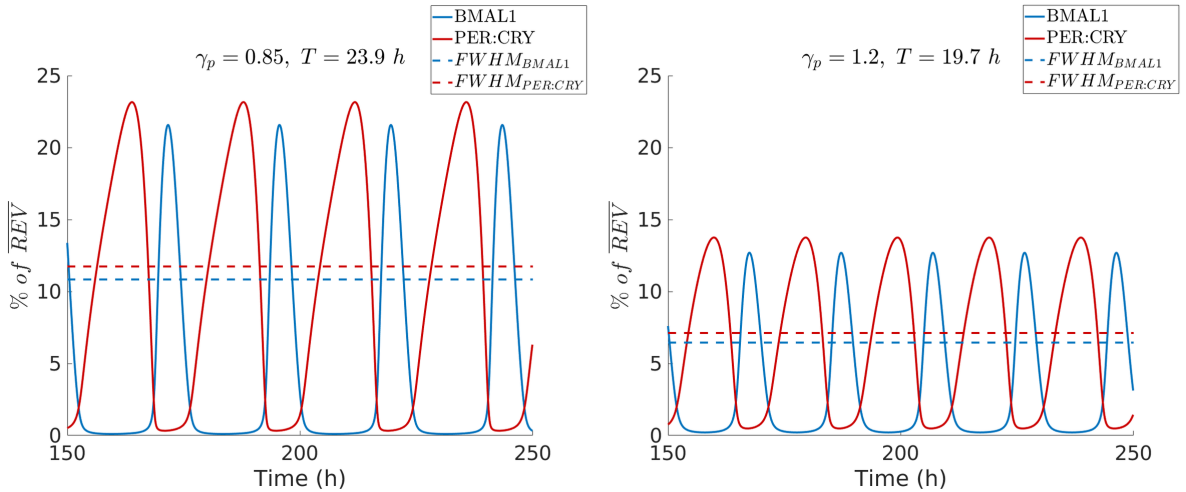


**Figure 18: Oscillation of BMAL1 and PER:CRY for two values of  $\gamma_p$ .** Changing  $\gamma_p$  from a  $CK\epsilon^{WT}$ -compatible period to a  $CK\epsilon^{\tau/\tau}$ -compatible period leads to similar decreases in BMAL1 and PER:CRY amplitude of oscillation and mean value, but to asymmetric changes in BMAL1 and PER:CRY FWHM as well as BMAL1 and PER:CRY phase differences. FWHM of PER:CRY decreases with  $\gamma_p$ , while FWHM of BMAL1 remains approximately constant. Furthermore, the peak of PER:CRY gets closer in time to the previous peak of BMAL1 with increasing  $\gamma_p$ , while the time between the BMAL1 peak and the previous PER:CRY peak doesn't change.